Textural Analysis of a Fibronectin Network during Early Embryogenesis

By

Rajprasad Loganathan

Submitted to the graduate degree program in the Department of Electrical Engineering and Computer Science and the Graduate Faculty of the University of Kansas in partial fulfillment of the requirements for the degree of Master of Science.

_____

Chairperson: Dr. Rongqing Hui

_____

Committee members Dr. Swapan Chakrabarti

_____

Dr. Brian Potetz

_____

Dr. András Czirók

Date defended: _____

The Thesis Committee for Rajprasad Loganathan certifies that this is the approved Version of the following thesis:

Textural Analysis of a Fibronectin network during Early Embryogenesis

_____

Chairperson: Dr. Rongqing Hui

Date approved: _____

Acknowledgments

I would like to thank Dr. Ron Hui, Dr. Charles Little, Dr. Brenda Rongish, Dr. Andras Czirok, Dr. Swapan Chakrabarti and Dr. Brian Potetz for their mentoring and full support in making my learning experience very interesting.

Abstract

Fibronectin is a major extracellular matrix molecular component that plays a critical role in embryonic cell motility and morphogenesis. During early development, the fibronectin molecular network is nearly ubiquitous in distribution across the entire embryonic volume. As a result, the embryonic fibronectin distribution is functionally relevant to both cell motility and organogenesis. Despite its biological importance, the structural attributes of embryonic fibronectin distribution are poorly understood. The textural features of an extracellular matrix network like that of fibronectin is not known.

By marking the embryonic tissue, obtained during specific stages of development, using fibronectin indirect immunofluorescence, fluorescent microscopy images capturing the embryonic fibronectin distribution were obtained. Using the properties of the gray scale co-occurrence matrix, textural attributes of a fibronectin network was derived for quail embryos during their early stages of morphogenesis. As a result, textural properties like inertia, correlation, uniformity, entropy and homogeneity were assessed for the medial (including the embryonic anteroposterior axis) and lateral (excluding the embryonic anteroposterior axis) fibronectin . The results not only demonstrated a noticeable heterogeneity of fibronectin textural properties across the embryonic regions examined, but also across the developmental stages that were studied. The spatial anisotropy and the temporal evolution across the developmental span in the textural attributes of embryonic fibronectin may have functional consequences for cell motility and morphogenesis.

With this thesis, textural analysis has found yet another application, viz. the study of the surface structural attributes of an extracellular matrix protein network in the context of developmental biology. The work presented in this thesis is the first of its kind in applying texture analysis with gray scale co-occurrence matrix method to study the spatial distribution of fibronectin matrix within a given stage of embryonic development and the temporal textural changes as the embryonic development progresses from stage 5 through stage 9.

Table of Contents

List of Figures

Chapter 1: Introduction

1.1 Motivation

The formation of a whole organism from the single cell, the fertilized egg, is nothing short of a marvel. The right combination of gene expression patterns, cell divisions, tissue movements and growth advance the development of an embryo. Along with cellular dynamics, the critical role of extracellular matrix (ECM), a highly organized multimolecular structure that is outside of cells, has recently been recognized in the orchestration of embryonic development. Among the many members of the family of ECM molecules, fibronectin particularly stands out as a very early structural component of the matrix.

It has been shown that in the absence of fibronectin, embryonic development is lethal [George, 1993, 1079]. Recent studies have clearly implicated the dynamics of fibronectin in early embryonic development [Zamir,2006,19806 ;Zamir,2008, e247; Czirok,2008,269]. The physical state of fibronectin affects the tissue morphogenetic processes in the early embryo [Rozario,2009,386]. These evidence on the role of fibronectin during embryonic development taken in the context of a cell's preference to move towards/away from matrix molecules depending on the mechanical attributes of the matrix molecules (durotaxis) [Lo, 2000, 144], suggests a role for the structural attributes of fibronectin in affecting the cell movements and hence embryonic development. As a result, characterization of the micron level structure of

fibronectin is necessary [Vakonakis, 2007, 578]. Characterization of the micron level structure could potentially elucidate the nature of the cellular interaction with ECM during embryonic development.

As an exploration towards the study of the micron level attributes of matrix structure, the investigation of the textural properties of fibronectin was carried out in this project. The analysis of fibronectin texture in multiple regions during embryonic development provides clue to the spatial heterogeneity of textural attributes even with respect to this one molecule and demonstrates the complexity of embryonic growth from the perspective of ECM dynamics.

Previous work has been done to characterize fibronectin network in cell culture in terms of the structural and functional properties of the matrix along with its effect on embryonic cell motility [Rovasio, 1983, 462; Duband, 1986, 160]. Few studies have also attempted to study the role of fibronectin in the early embryo, particularly during gastrulation (the process which changes an embryo from being a single layered ball of cells to become a two layered tube of cells, and subsequently a three germ layered organism, Appendix) [Zamir,2006,19806 ;Zamir,2008, e247; Czirok,2008,269]. Although these studies give us an introduction to the nature of early embryonic fibronectin dynamics, there has not been any exploration of the structural attributes of a fibronectin network. For example, during gastrulation cells move from more medial regions of the embryo towards the lateral regions on a

fibronectin network along their trajectory. Whether the structural properties are isotropic with respect to cell motility is unclear.

In order to characterize the micron level attributes of fibronectin network in the early stages of embryonic development, the textural properties of the fibronectin matrix from stages 5 through 9 in quail embryos were studied. A brief review on staging embryos and the basic biology of the methods involved in the research approach are provided in the background section.

Chapter 2: Background

Motivation to Study the Avian Embryo

Bird embryos develop in the egg (i.e., outside the mother) and hence allow detailed investigations of cell biology without compromising the health of the mother. In addition, the development of the embryo can be achieved by incubating the eggs in an external temperature controlled chamber (incubator). Moreover, the cellular and molecular events of early embryogenesis in avian embryos closely resemble the early cellular and molecular events in human embryonic development.

Stages of Embryonic Development

By incubating the eggs at approximately 38 °C for a specific duration, we can get the desired amount of development. This process is called staging. Stages 1 through 10 correspond to the early stages of embryonic development in the chick embryo when the embryo undergoes remarkable changes in morphology from being a single layer of cells to a three germ layered embryo as shown in figures 1 and 2. The three germ layers later give rise to the entire tissues and organs of the body (Appendix).

Figure 1: Developmental stages 1 through 3 from a chick from the reprinted version (1991) of the original article (1951) by Hamburger and Hamilton(HH).

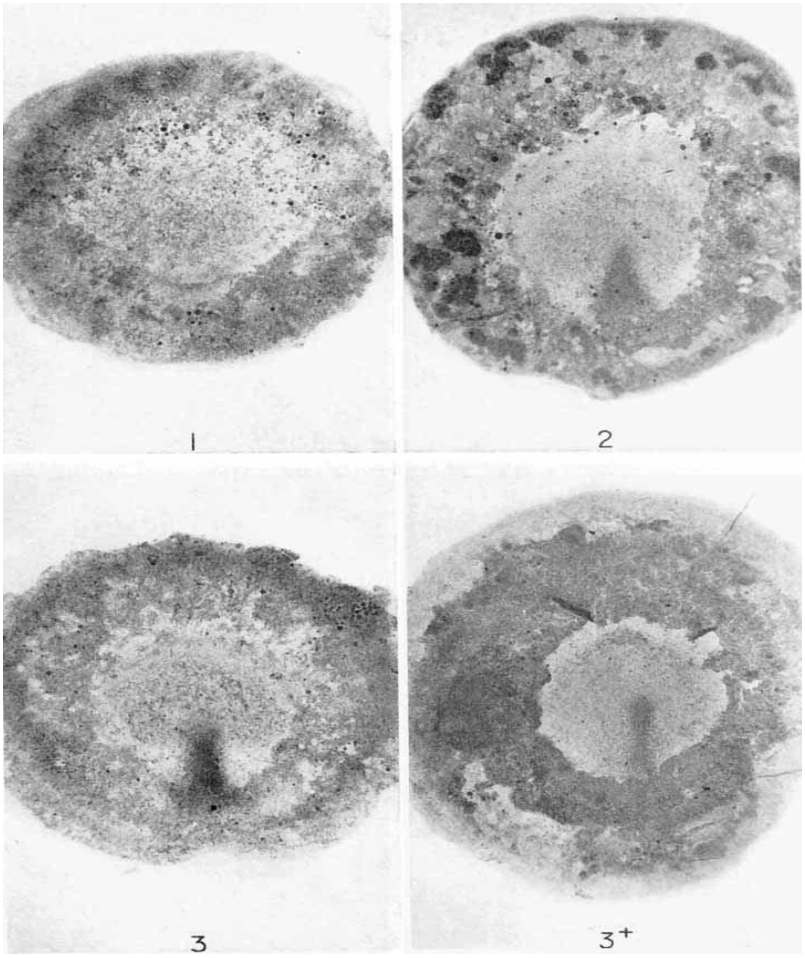

Figure 2: Developmental stages 4 through 10 from a chick from the reprinted version (1991) of the original article (1951) by Hamburger and Hamilton

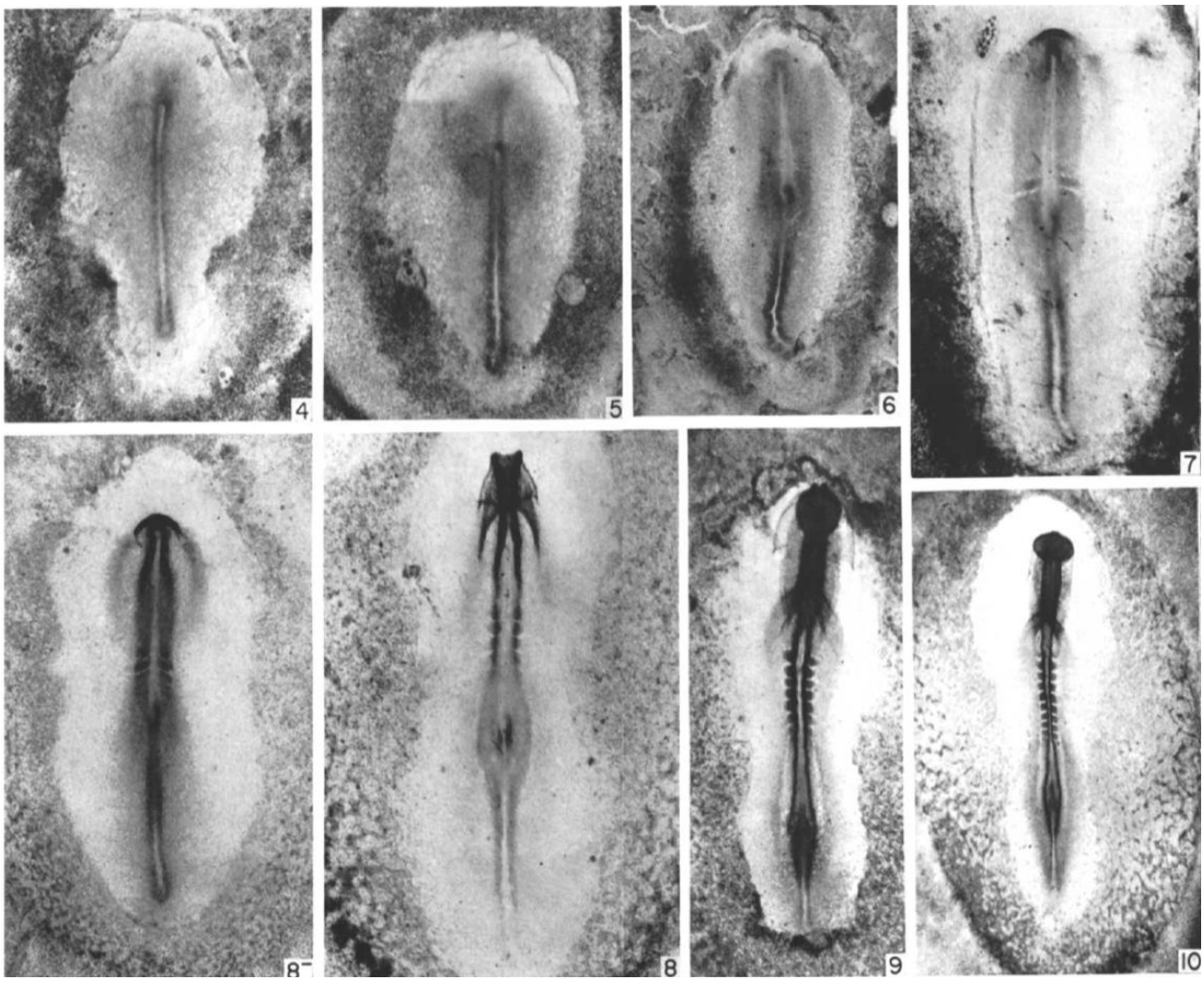

Fibronectin

Fibronectin molecule (a protein) is a strand of independent, globular domains connected by short, flexible segments. The length of the strand is about 140 nm and the diameter is about 2 nm. Based on previous studies, the following protein level schematic of the

fibronectin is presented (figure3). The major part of the molecule is organized in to three types of homologous repeats. Type 1 repeat is about 45 amino acid residues long, type 2 repeat is 60 residues long and type 3 repeat is 90 residues long. Studies also show the capacity of the molecule to interact with a variety of ligands (for e.g., fibrin, heparin, bacteria, cells and collagen).

Figure 3: Schematic of a fibronectin chain (two chains connected by a disulfide bond makes the entire molecule) with type 1 (red), type 2(green) and type 3 (blue) repeats

Fibronectin is present in the embryo as early as stage 2 [Vakaet, 1962, 38 ; Duband, 1982,337 ; Sanders, 1982, 155; Mitrani, 1982, 197; Zamir, 2008,e247]. During gastrulation (see appendix), the cells of mesoderm that migrate out laterally from the primitive streak (see appendix) remain closely associated with a fibronectin containing matrix network. After gastrulation, when the neural crest cells detach from the neural tube and migrate to various areas of the embryo on a fibronectin containing matrix network, in order to form the peripheral and autonomic nervous system, endocrine and craniofacial tissues [Newgreen, 1980, 269; Duband, 1982, 308; thiery, 324; Vincent, 1984, 468; Bronner-Fraser, 1985, 610]. Other cell types including the primordial germ cells [Critchley,1979, 498], muscle cells or myoblasts [Chiquet, 1981, 220], hemopoietic and endothelial cells [Risau, 1988, 441; Drake,1990, 309; Rupp,2001,566] also migrate along a fibronectin rich matrix network in vertebrates.

In fact, the endothelial cells that assemble to form the primitive blood vessels in the embryo closely follow the fibronectin matrix network. The fibronectin network in a stage 8 embryo spreads in the form of a polygonal array (figure 4) much like the primitive blood vessels. Consequently, fibronectin plays an important role in the early embryo for cell motility, cell assembly or anchorage and morphogenesis. Although all these processes (cell motility, assembly & morphogenesis) have been extensively studied in the past from the point of chemotaxis [Thiery, 1984, 1; Böttcher RT, 2005, 63; Affolter M,2005, 19; Vasiev, 2010,e10571], very few studies [Poole, 1982, 144; Lo, 2000, 144]suggested the possibility of cell/matrix interaction in the form of haptotaxis or durotaxis,i.e., the phenomenon that describes the cell-matrix interactions based on the changes in physical properties of the substrate (matrix) and the consequent cellular behavior.

Figure 4: Fibronectin network in a stage 9 embryo is nearly ubiquitous across the entire embryonic volume

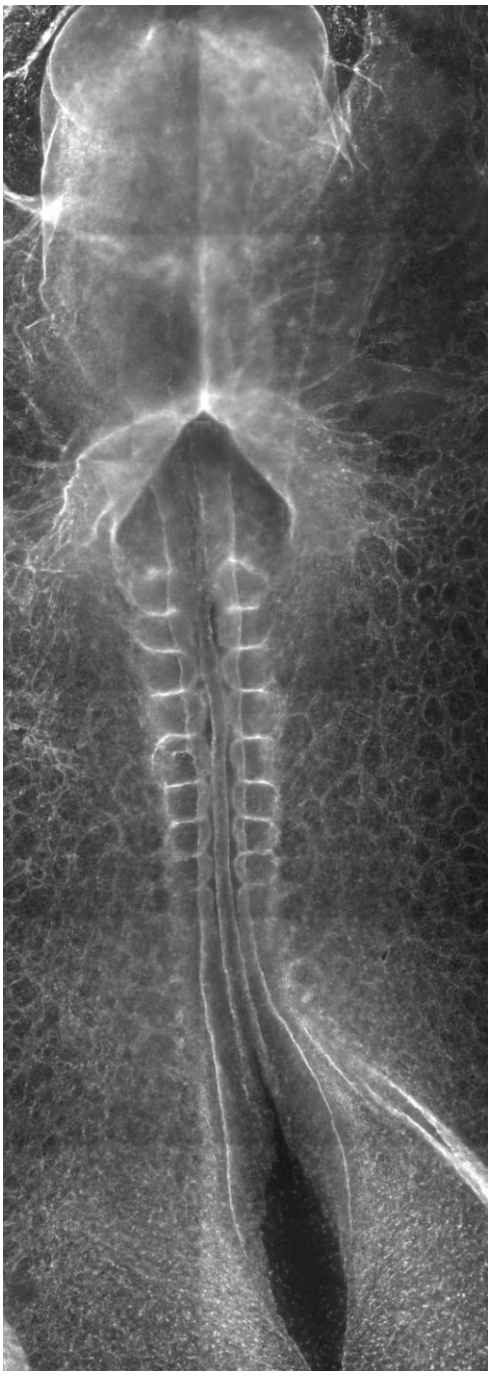

Textural Analysis

According to the Merriam-Webster dictionary online, the definitions of the word texture ranges from "something composed of closely interwoven elements," to "basic scheme or structure." Among those definitions are the following: a) the disposition or manner of union of the particles of a body or substance and b) the visual or tactile surface characteristics and appearance of something. With respect to the analysis of fibronectin in this thesis, it could be stated that the textural analysis captures the visual surface characteristics of the protein network (disposition of the fibronectin molecules to form a tissue level architecture) obtained through a variety of standard measures. We imply (assume) that these measures of visual surface characteristics perhaps capture (computationally), features that translate/correspond to a tactile representation from the view point of cellular interactions with the fibronectin matrix. If we follow this line of thought, then the textural descriptions of a protein network such as fibronectin during early development have biological implications.

A successful vision system uses textural cues to identify the objects in natural world. The fundamental question that led to the study of textures in detail is this: What are the visual processes that allow one to separate figure from ground using the texture cue? [Tuceryan, 1998, 207]. The initial framework that attempted to explain human vision using textural cues later became the basis for textural analysis as an important and useful area of study in machine vision. The performance of various algorithms was evaluated against the performance of human visual system doing the same task. The

initial work was performed in the field by Julesz [Julesz, 1962, 84] that proposed the theory of textons (visual events such as collinearity, terminations, closure, etc.) and applied the theory to machine vision [Julesz, 1981, 91]. According to the theory, two textures are not preattentively discriminable (effortlessly discriminable) if their second-order statistics are identical.

The standard view in textural analysis synthesized by Haralick from a wide range of preliminary work in the field includes both structural and statistical approaches to the analysis of texture based on imagery of objects [Haralick, 1979, 786]. Texture was defined formally as an organized area phenomenon that depended primarily on the tonal primitives of images. Tonal primitives, in turn, were defined as maximally connected set of pixels (regions) with properties that allowed description in terms of average tone, or maximum and minimum tone of its region.

In a way, it could be said that texture and tone are two sides of the same coin. If we take for example, a small region of the image under consideration, and observed very little variation of tonal primitives in that region we would then conclude that the dominant property of that region is tone. On the contrary, if that small region consisted of wide variations in the tonal primitives, we would conclude that the dominant property of that region is texture. These observations indicate that an increase in the number of distinguishable tonal primitives within a defined region of interest (ROI) leads to an increase in textural properties in that ROI . If these attributes persist across the entire image, the image texture becomes conspicuous. The level of randomness in the spatial

distribution of distinguishable tonal primitives determines the qualitative nature of the texture. A random distribution in the presence of wide gray tone variation between primitives leads to a fine texture. A less random (or more definite) distribution of tonal primitives in the presence of tonal regions that involve more resolution cells (pixels) will result in a coarser texture. Other qualitative descriptions of texture include smoothness, granulation, randomness, lineation, irregular, hummocky etc. Unfortunately, a definitive translation of these qualitative attributes of texture in to computational variables (and vice versa) is unreliable from early research. As a result, a relative definition of smoothness vs. coarseness is the only qualitative description used in the analysis presented in this thesis.

Two basic dimensions define a decomposable texture: a) the tonal primitives themselves (i.e., the primitives out of which the image texture is composed) and b) the spatial organization of the tonal primitives (i.e., the spatial dependence or interaction between the tonal primitives). These dimensions result in descriptions of an image texture on the basis of a) number of its primitives, b) the types of its primitives and c) the spatial organization of its primitives.

As mentioned earlier, two common approaches for textural analysis exist: a) structural approach and b) statistical approach. The structural approach is based on the view that the textures under analysis are composed of a spatially repeating primitive arrangement (i.e., the existence of a spatial periodicity). Under such circumstances, if we wanted to describe the texture structurally, we must also describe the primitives and the placement

rules governing those primitives [Carlucci, 1972, 53]. These primitives could be modeled on, for example, repeating line segments, open polygons and closed polygons where the placement rules are provided syntactically in a graph-like language.

Biological entities such as a protein network like fibronectin present favorably to a probabilistic description of texture. As a result, textural analysis of fibronectin network was pursued using the statistical approach in this thesis. There are a number of statistical methods widely used in the description of textures. We briefly discuss those and elaborate on the specifics of the method utilized in this thesis at the end of this chapter.

1. Autocorrelation function

   The autocorrelation function provides us information about the size of the tonal primitives (gray tones). The spatial organization of the tonal primitives is characterized by the correlation coefficient which is a measure of the linear dependence one pixel on another. Relatively large tonal primitives on the image result in an autocorrelation drop off slowly with distance (coarse texture) while relatively small tonal primitives lead to a quick drop off with respect to distance (smooth texture)

2. Optical processing methods

   The optical processing methods of texture classification rely on the fact that the light amplitude distributions at the front and back focal planes of a lens are Fourier

transforms of one another. The light distribution (from the lens) is known as the Fraunhofer diffraction pattern that facilitate two dimensional frequency analysis of images and pattern recognition based on the diffraction patterns which are utilized as the basis for texture classification.

3. Digital transform methods

The digital transform methods of texture analysis use the Fourier transform, Hadamard transform etc. on the images to obtain the basis vectors in the transform domain that relate to the spatial frequency (sequency). The tonal primitive in these sequency models is the gray tone. These methods also use the power spectral density (Fourier transform of the autocorrelation) to derive textural information.

4. Textural edgeness

While the autocorrelation function, optical and digital transform methods reference texture to sequency, the textural edgeness method treats texture as edgeness per unit area. In this scheme, a measure of texture can be obtained by computing the sum of the absolute value of the differences between diagonally opposite neighboring pixels (the quick Roberts gradient) in pairs of non-overlapping neighborhoods bordering the resolution cell to detect edgeness.

5. Mathematical morphology

   This structural element approach to texture is based on the idea that a structural element can be defined as a set of resolution cells constituting a specific shape and to generate a new binary image by translation of the structural element through the image and erosion by structural elements the figures formed by contiguous resolution cells having the value 1. The generalized covariance function is then used on the structural elements (that define the morphology of the object of study) to obtain the textural information in the image.

6. Spatial gray-tone dependence: co-occurrence

   Julesz [Julesz, 1962, 84] was the first to use gray tone spatial dependence co-occurrence statistics in texture discrimination experiments. The procedure rests on the idea that texture is concerned with the spatial distribution and spatial dependence of gray tones in a local field on the image. Some of the features computed from the co-occurrence probabilities are uniformity or energy, entropy, contrast, maximum probability, inverse difference moment, correlation and probability of a run length.

7. Textural transform

   In this method, an image J is constructed such that the gray tone J (i, j) at resolution cell (i, j) indicates how common the texture pattern is in and around the resolution cell (i, j) of an image I where Image J is the textural transform of image I.

8. Generalized gray-tone spatial dependence models for texture

   In this approach, for a specific neighborhood and a sub-image, it is possible to estimate the joint probability distribution of the gray tone of the neighborhood in the sub-image. The generalized gray-tone spatial dependence model for texture is based on this joint distribution. The neighborhood is the primitive and the arrangement of its gray tones is the property. The texture characterization is given by the joint distribution of the gray tones in the neighborhood.

9. Run lengths

   A gray level run length primitive is given by a maximal collinear connected set of pixels all having the same gray tone. Gray level run lengths are characterized by the gray tone of the run, the length of the run, and the direction of the run. Some of the useful statistics that are obtained from the run lengths are short run emphasis inverse moments, long run emphasis moments, gray level non-uniformity, run length non-uniformity and fraction of image in runs.

10. Autoregression models

    Autoregression model for texture exploits the property of the autocorrelation function which describes the linear dependence one pixel of an image has on another. Both texture segmentation and texture synthesis applications employ the autoregression models.

11. Mosaic texture models

These texture models tessellate (tiling of a plane) an image into regions and assign a gray level to the region according to a specified probability density function. Some of these models are the occupancy model, the Johnson-Mehl model, the Poisson line model and the Bombing model.

The gray tone co-occurrence method

The autocorrelation functions, optical processing methods and digital transforms are spatial frequency approaches to determining the texture. The major disadvantage of these methods is their invariance under a monotonic transformation of gray tone. Although probability quantization techniques reduce the invariance, it also leads to a loss of gray tone precision. The structural elements method places the emphasis on the shape aspects of the tonal primitives while the autoregressive models are appropriate only for the analysis of microtextures. Meanwhile the gray tone co-occurrence probabilities characterize the spatial interrelationships of gray tones with invariance under monotonic transformations while providing a set of estimates on the statistics that underlie the textural characteristics of the object. As a result, this method is described in detail and is used to extract the textural information from a fibronectin network in this thesis.

The spatial gray-tone dependence (co-occurrence) method is based on the spatial dependence among the gray tones in a local area that was first used by Julesz [Julesz, 1962, 84] in texture discrimination experiments. Haralick [Haralick, 1972] used the gray tone co-occurrence matrix to compute textural features of images. The following description on the method is based on the work by Haralick.

Let us suppose that the area of interest is rectangular and has N_c resolution cells in the horizontal direction and N_r resolution cells in the vertical direction with the gray tone appearing in each of the resolution cell quantized to Ng levels. Hence, $L_c = \{1, 2, \ldots, N_c\}$ is the horizontal spatial domain and $L_r = \{1, 2, \ldots, N_r\}$ is the vertical spatial domain and $G = \{1, 2, \ldots, N_g\}$ is the set of Ng quantized gray tones. The image I can then be given as a function that assigns some gray tone G to each resolution cell or pair of coordinates in L_r x L_c; I: $L_r x L_c \rightarrow G$.

The gray tone co-occurrence can be given by a matrix of relative frequencies P_{ij} with which two neighboring resolution cells separated by a distance d occur on the image with gray tones i and j respectively. For example, consider a 4x4 image given as $L_y = \{1, 2, 3, 4\}$ and $L_x = \{1, 2, 3, 4\}$ shown below

(1, 1)	(1, 2)	(1,3)	(1,4)
(2, 1)	(2, 2)	(2, 3)	(2, 4)
(3, 1)	(3, 2)	(3, 3)	(3, 4)

(4, 1)	(4, 2)	(4, 3)	(4, 4)

The set of all distance 1 horizontal neighboring resolution cells on this 4x4 image is given by

$R_H = \{(k, l), (m, n) \in (L_y \times L_x) \times (L_y \times L_x);\ \|k - m = 0\|,\ \|l - n = 0\|\}$

R_H for this example is shown as

(1, 1), (1, 2)	(1, 2), (1, 1)	(1, 2), (1, 3)	(1, 3), (1, 2)
(1, 3), (1, 4)	(1, 4), (1, 3)	(2, 1), (2, 2)	(2, 2), (2,1)
(2, 2), (2, 3)	(2, 3), (2, 2)	(2, 3), (2, 4)	(2, 4), (2, 3)
(3, 1), (3, 2)	(3, 2), (3, 1)	(3, 2), (3, 3)	(3, 3), (3, 2)
(3, 3), (3, 4)	(3, 4), (3, 3)	(4, 1), (4, 2)	(4, 2), (4, 1)
(4, 2), (4, 3)	(4, 3), (4, 2)	(4, 3), (4, 4)	(4, 4), (4, 3)

For angles quantized to 45^o intervals, the un-normalized frequencies are given by the following:

$P(i, j, d, 0^o) = \#\{((k, l), (m, n)) \in (L_r \times L_c) \times (L_r \times L_c);\ k - m = 0,\ \|l - n\| = d;\ I(k, l) = i\ \&\ I(m, n) = j\}$

$P(i, j, d, 45^{o}) = \#\{((k, l), (m, n)) \in (L_r \times L_c) \times (L_r \times L_c); (k - m = d, l - n = -d) \text{ or } (k - m = -d, l - n = d); I(k, l) = i \ \& \ I(m, n) = j\}$

$P(i, j, d, 90^{o}) = \#\{((k, l), (m, n)) \in (L_r \times L_c) \times (L_r \times L_c); \|k - m\| = d, l - n = 0; I(k, l) = i \ \& \ I(m, n) = j\}$

$P(i, j, d, 135^{o}) = \#\{((k, l), (m, n)) \in (L_r \times L_c) \times (L_r \times L_c); (k - m = d, l - n = d) \text{ or } (k - m = -d, l - n = -d); I(k, l) = i \ \& \ I(m, n) = j\}$

where # refers to the number of elements in the set.

For demonstration purposes, let us consider a 4 x 4 image with four gray tones ranging from 0 to 3, shown as below:

0	0	1	1
0	0	1	1
0	2	2	2
2	2	3	3

The position values of the gray tone co-occurrence matrix for a given distance or angle depends on the number of gray tones in the image, and for this example it is:

	0	1	2	3
0	#(0, 0)	#(0, 1)	#(0, 2)	#(0, 3)
1	#(1, 0)	#(1, 1)	#(1, 2)	#(1, 3)
2	#(2, 0)	#(2, 1)	#(2, 2)	#(2, 3)
3	#(3, 0)	#(3, 1)	#(3, 2)	#(3, 3)

For the distance of 1 and various angles (0^o = **h**orizontal; 45^o = **r**ight **d**iagonal; 90^o = **v**ertical; 135^o = **l**eft **d**iagonal), the spatial co-occurrence calculations for the above example are given as following:

P_H =

4	2	1	0
2	4	0	0
1	0	6	1
0	0	1	2

P_{RD} =

4	1	0	0
1	2	2	0
0	2	4	1
0	0	1	0

P_V =

6	0	2	0
0	4	2	0
2	2	2	2
0	0	2	0

P_{LD} =

2	1	3	0
1	2	1	0
3	1	0	2
0	0	2	0

For example, the element in the (2, 2)th position of the distance 1 horizontal P_H matrix (highlighted green) is the total number of times two gray tones of value 2 and 2 occurred horizontally adjacent to each other (highlighted yellow). To determine this number, we count the number of pairs of resolution cells in R_H such that both the first and second resolution cell pairs have a gray tone value of 2. In this case, the total number is 6 which fills the (2, 2) position in the P_H matrix.

Using the gray tone co-occurrence matrix various features can be computed that provide textural information about the image regions of interest. The following features are commonly used in textural analysis:

Energy or Uniformity	$\sum\sum P_d^2(i, j)$ over all i's and j's
Entropy	$-\sum\sum P_d(i, j)\log P_d(i, j)$ over all i's and j's
Contrast	$\sum\sum (i-j)^2 P_d(i, j)$ over all i's and j's
Homogeneity	$\sum\sum P_d(i, j)/(1 + \|i - j\|)$ over all i's and j's
Correlation	$\sum\sum (i - \mu_x)(j-\mu_y)P_d(i, j)/(\sigma_x\sigma_{y)}$ over all i's and j's

In summary, we are able to say that texture is a contextual property of areas and its definition must involve gray values in a spatial neighborhood. Thus spatial gray-tone co-occurrence matrices are reasonable statistical textural analysis tools.

The interrelationship between the various second-order statistics and the input image are summarized in figure 5.

Figure 5: Interrelationship between various second order statistics and the original image during texture analysis based on [Tuceryan, 1998, 207]

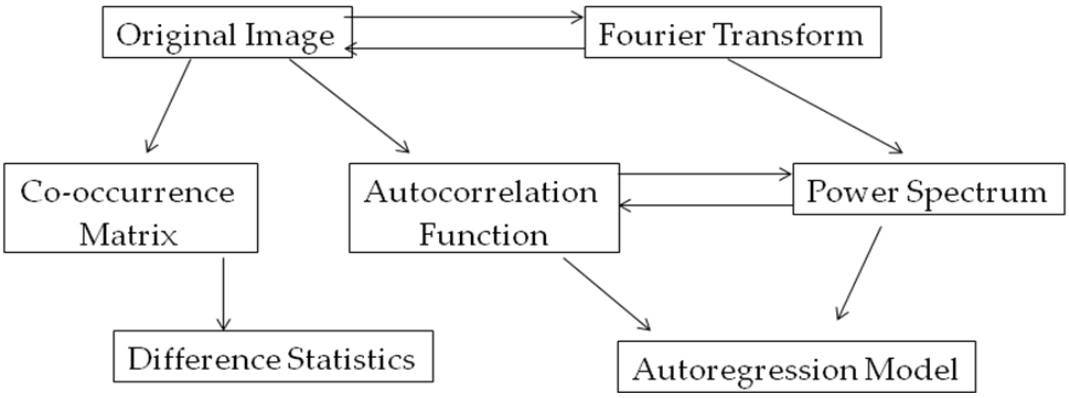

Chapter 3: Related Work

Texture analysis has found several applications since its origin in the field of visual psychophysics. Importantly, the role of texture analysis has gradually increased in the following application areas: a) automated inspection, b) medical image processing, c) document processing and d) remote sensing.

Automated inspection: Applications include defect detection in images of textiles and inspection of carpet wear and automobile paints. Using signal processing methods (filterbanks) to filter the images, Dewaele *et al.* [Dewaele, 1988, 56] computed the texture features from the filtered images. They also used a Mahalanobis distance classifier to classify defective areas. In the study by Conners *et al.* [Conners,1983, 573], texture analysis methods were used for automatic inspection of lumber wood. Tonal features such as mean, variance, skewness and kurtosis of gray levels along with texture features computed from gray level co-occurrence matrices were used in analyzing the images of wood. In the area of quality control, Siew *et al.* [Siew, 1988, 105] used second-order gray level dependent statistics and first-order gray level difference statistics to compute the textural features of carpet wear successfully. Furthermore, Jain *et al.* [Jain, 1990, 1] used a filter bank composed of Gabor filters to compute the textural features for the purpose of automatic classification of the painting quality of metal surfaces. Other applications of texture analysis of this kind extend to the food processing industry.

Medical image processing: The most common application of texture analysis in medical image processing has been to differentiate the pathological tissue from normal tissue. In fact, it has been shown that pathologies that involve an excessive deposition of extracellular matrix in tissue (for example, interstitial fibrosis of lung) produce images that show textural changes more readily than clearly delineated lesion upon analysis [Sutton, 1972, 667]. Doyle et al. [Doyle, 2008, 496] extracted both textural and graph features to formulate the use of computer aided diagnosis of breast cancer from the analysis of mammography. The textural features that were used include the gray level features, Haralick features and Gabor filter features. In another study, Doyle et al. [Doyle, 2007, 1284] used a similar methodology to detect prostate cancer using architectural and textural features. They described a co-adjacency matrix analogous to the gray scale co-occurrence matrix. The diagonally symmetric co-adjacency matrix described the spatial relationships between each pairs of glands seen on the images of the affected tissue. The textural features were weighted heavily in the algorithm used for discrimination of tissue types in this study.

Document Processing: One of the useful applications of machine vision is in the area of document processing and character recognition. In order to identify regions of interest on a document, texture segmentation techniques could be used [Jain, 1991, 1167]. The segmentation was obtained using three classes of textures: a) for text regions, b) for uniform regions that form the background and c) for transition areas between the two types of regions (text and uniform background).

Remote Sensing: An extensive literature exists on the development of texture analysis techniques for the purpose of remote sensing, for example, land use classification where homogeneous regions with different types of terrains (such as wheat, bodies of water, buildings, roads, etc.) need to be identified. Haralick et al. [Haralick, 1973, 610] in one of the earliest studies of this kind used gray level co-occurrence features to analyze remotely sensed images. They computed gray level co-occurrence features for a distance of one with four directional quantizations. Textural features have also been computed from synthetic aperture radar images (SAR) using texture features computed from gray level co-occurrence matrices [Rignot, 1990, 1979]. Du [Du, 1990, 1983] used texture features obtained from Gabor filters to segment SAR images into the following categories: water, new forming ice, older ice, and multi-year ice. Spectral textural features have also been used to segment SAR images [Lee, 1990, 2005].

As seen in this section, a variety of application areas have benefited from texture analysis on the images of objects/regions of interest. Meanwhile, this thesis extends the utilization of texture analysis to the study of an extracellular matrix protein network (fibronectin) during early stages of embryogenesis in an attempt to characterize the fibronectin network in textural terms.

Chapter 4: Methodology

Embryo staging and preparation

Locally raised fertilized quail eggs (*Coturnix coturnix japonica*, Ozark Eggs, Stover, MO) were incubated for approximately 20–30 h at 38 °C to obtain HH stages 5 through 9 embryos [Hamburger, 1992, 231]. The embryo was dissected from the egg, mounted on filter paper rings, placed ventral side up on a semi-solid mixture of agar/albumen (egg whites) (modified after the method of New [New, 1955, 326; Little, 2000, 183; Chapman,2001, 284]), and cultured at 38 °C until approximately HH stage was obtained.

Immunofluorescent labeling of fibronectin

The embryos were fixed with 4% paraformaldehyde and dehydrated and rehydrated with a series of ethanol and embryonic phosphate buffered saline (EPBS) incubations and wash. Prior to immunolabeling the vitelline membrane was removed from the specimens to avoid auto fluorescence and non-specific antibody interactions. Immunolabeling was carried out on the fixed specimens using two separate antibodies. The primary antibody specifically recognizes the fibronectin and a generic secondary antibody recognizes the IgG portion of the primary antibody. The secondary antibody was conjugated to a fluorescent marker (Alexa-555) thus allowing fluorescent microscopy capture of the fibronectin network. The immunolabeling procedure was carried out as follows: After the last wash with EPBS 400-500 μL of 3% bovine serum albumin was added to the specimen to block the "non-antigenic" proteins for at least 1h

on a rocker. The primary antibody to fibronectin, B3D6 (Developmental Studies Hybridoma Bank, University of Iowa), was prepared in BSA solution at a 1:10,000 dilution. The BSA blocking solution was removed and 500 μ L of primary antibody solution was added to the specimens and incubated at 4 °C. After four hours of incubation, the primary antibody was removed and the specimens were washed three times, for at least 30 minutes each, with ~1 mL of PBS+azide. Following the wash, ~ 300 μL of secondary antibody conjugated to alexa-555 fluorochrome was added to the specimens and incubated overnight in dark at 4 °C. After the secondary incubation, the specimens were washed three times, for at least 30 minutes each, with ~1 mL of PBS + azide for mounting and viewing.

Image Acquisition

Images were acquired with a Nikon eclipse TE300 microscope equipped with a spot RTKE camera (Diagnostic instruments, Inc., Sterling Heights, MI) using a 10x objective. Regions of interest were captured under two categories in all the specimens across all the stages: 1) Medial (regions including the primitive streak in the early stages, or somites in the later stages) and 2) Lateral (regions that are adjacent to the streak/somites but lateral and hence do not include the primitive streak or somites).

Image processing

The stored tiff files were preprocessed in image J [http://rsbweb.nih.gov/ij/] (a freely downloadable Java based image processing environment), a widely used image

processing program in the biomedical sciences. The preprocessing involved background subtraction to view the fibronectin fluorescence. A standard cropping of the region of interest under actual pixel view to obtain a 429 x 510 array was performed with Adobe photoshop elements 6.0. The preprocessed images were then taken to matlab for texture analysis using the gray level co-occurrence matrix (GLCM). The texture parameters were obtained from the GLCM as a function of 16 offsets, four each at 0^{o}, 45^{o}, 90^{o} and 135^{o}. The entropyfilt function was utilized to obtain the local entropy maps of the fibronectin networks. The following textural features were derived:

a) Contrast (measures the local variations in the gray-level co-occurrence matrix)

b) Correlation (measures the joint probability occurrence of specified pixel pairs)

c) Energy (provides the sum of the squared elements in the GLCM. Also known as uniformity or the angular second moment)

d) Entropy (calculates the local entropy of the grayscale image. Entropy is the statistical measure of randomness)

e) Homogeneity (Measures the closeness of the distribution of elements in the GLCM to the GLCM diagonal)

Statistical analysis for entropy measures was performed with Sigmaplot version 11.

Chapter 5: Experimental Work

The following representative images provide the details obtained from the immunofluorescent micrographs of embryos probed with fibronectin antibody.

As mentioned earlier, the medial matrix network includes the primitive streak (future anteroposterior axis of the embryo) and the lateral matrix network does not.

In figure 6, which is from the stage 5 embryo, the medial firbronectin network is exposed and in figure 7, the lateral network is captured. The following morphological features qualitatively describe the visual arrangement of fibronectin at stage 5: the medial distribution is sparse whereas the lateral distribution is less sparse with fibers oriented in no preferred direction.

Figure 6: The medial distribution of fibronectin network in a stage 5 embryo

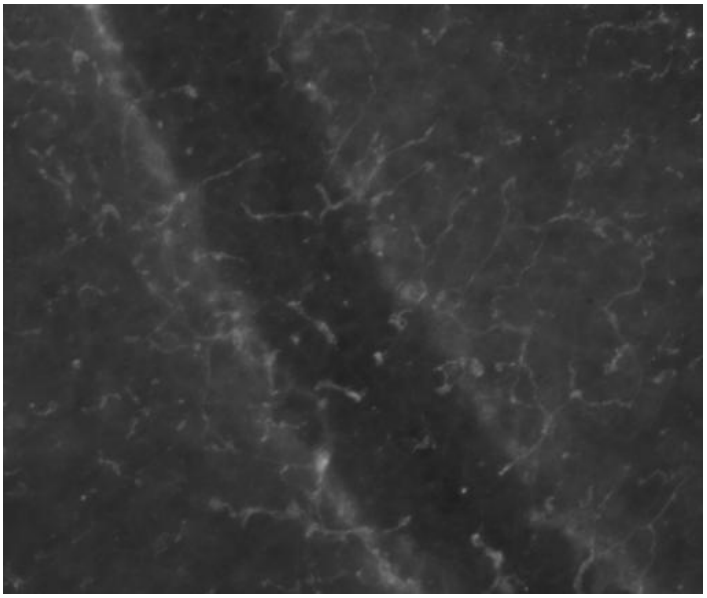

Figure 7: The lateral distribution of fibronectin network in a stage 5 embryo

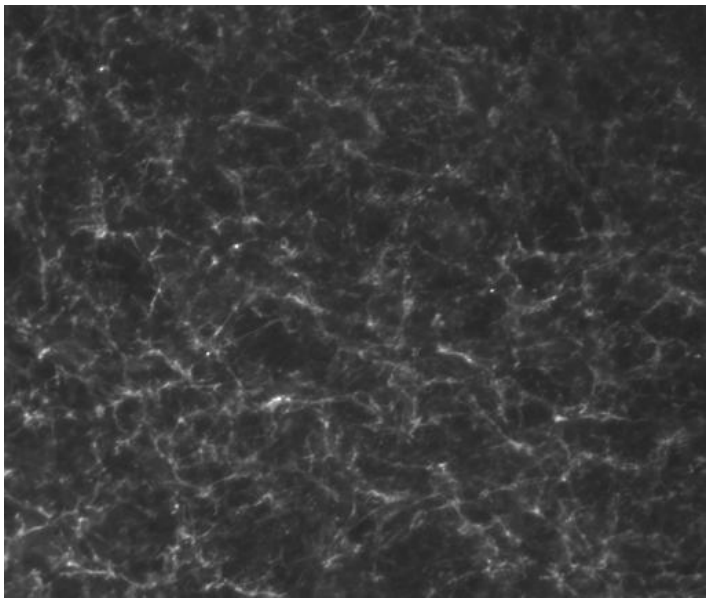

During stage 6 , the medial fibronectin network (figure 8) is thickened and more organized compared to stage 5, whereas the lateral matrix distribution at stage 6 (figure 9) is mostly similar to the morphology seen during stage 5.

Figure 8: The medial distribution of fibronectin network in a stage 6 embryo

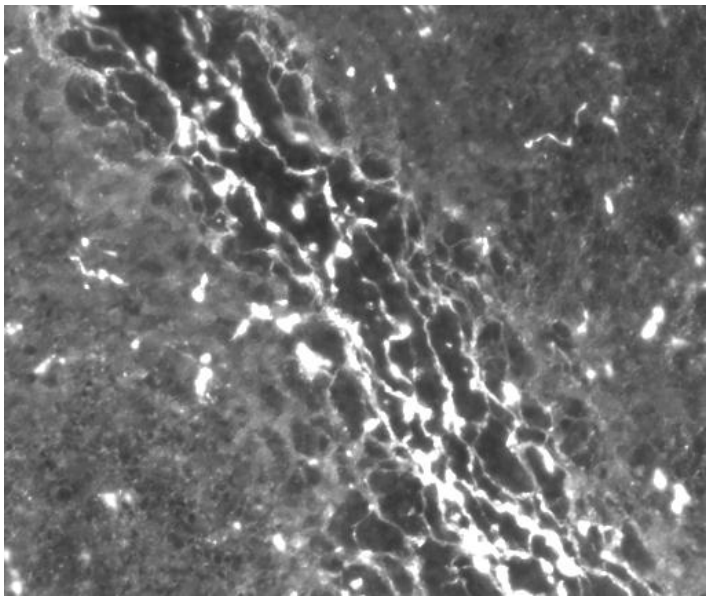

Figure 9: The lateral distribution of fibronectin network in a stage 6 embryo

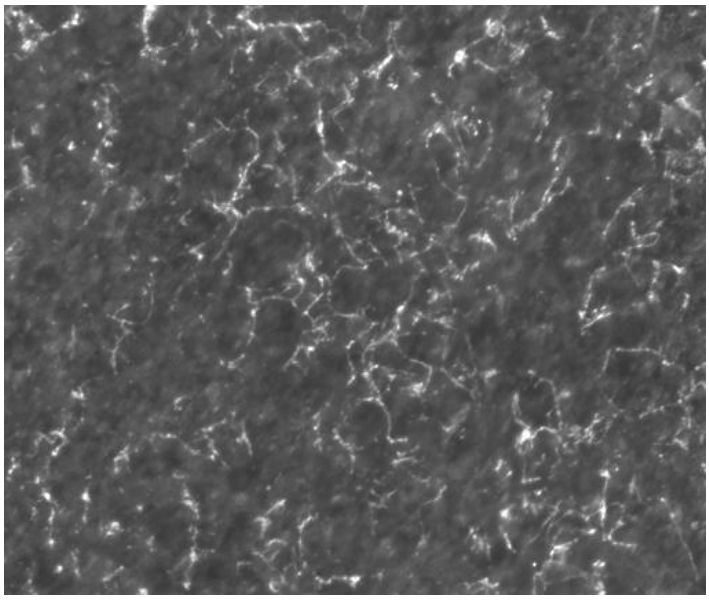

The thickening of medial fibronectin seen at stage 6 fails to proceed through stage 7. At this stage, a noticeable sparseness of fibronectin that is nevertheless filamentous (figure 10) covers part of the primitive streak and is supported by a dense network adjoining the streak. Meanwhile, the lateral network shows an uneven distribution of fibronectin structured like a mat (figure 11).

Figure 10: The medial distribution of fibronectin network in a stage 7 embryo

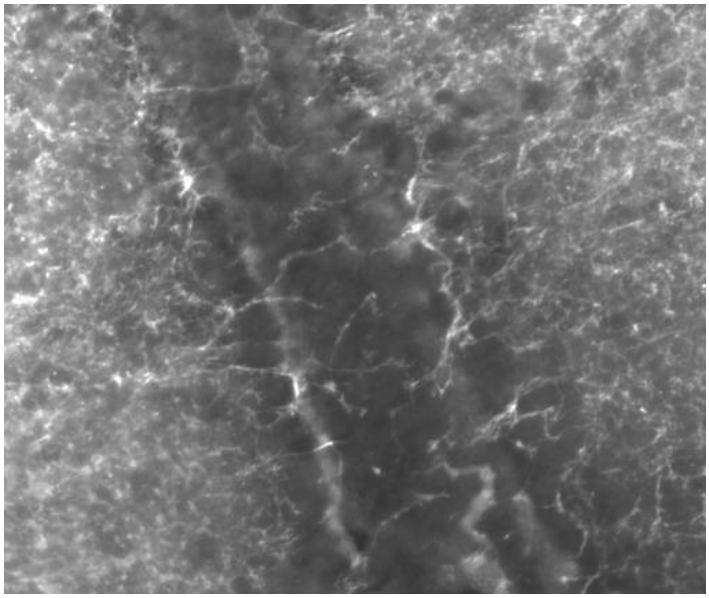

Figure 11: The lateral distribution of fibronectin network in a stage 7 embryo

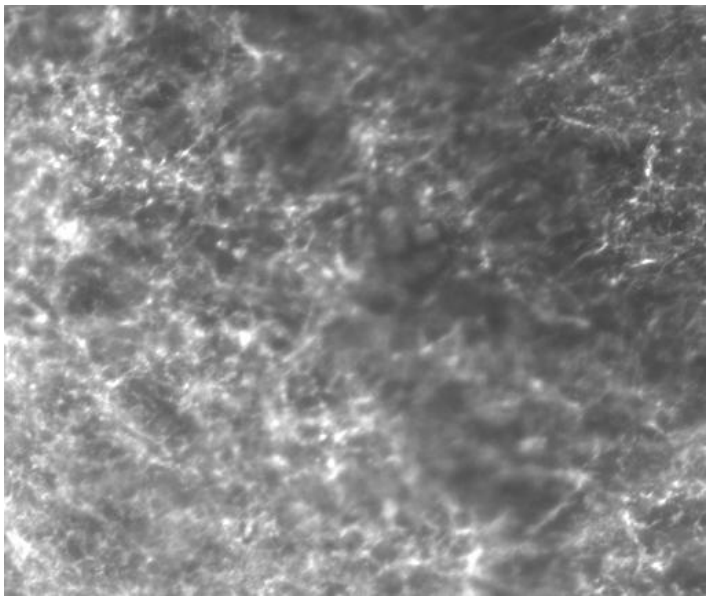

During stage 8, the medial distribution of fibronectin is mainly from the consolidated fiber formations of the somites (figure 12). Meanwhile, the lateral distribution shows beginning signs of an orderly arrangement, presumably playing a role in the formation of the first blood vessels (figure 13).

Figure 12: The medial distribution of fibronectin network in a stage 8 embryo

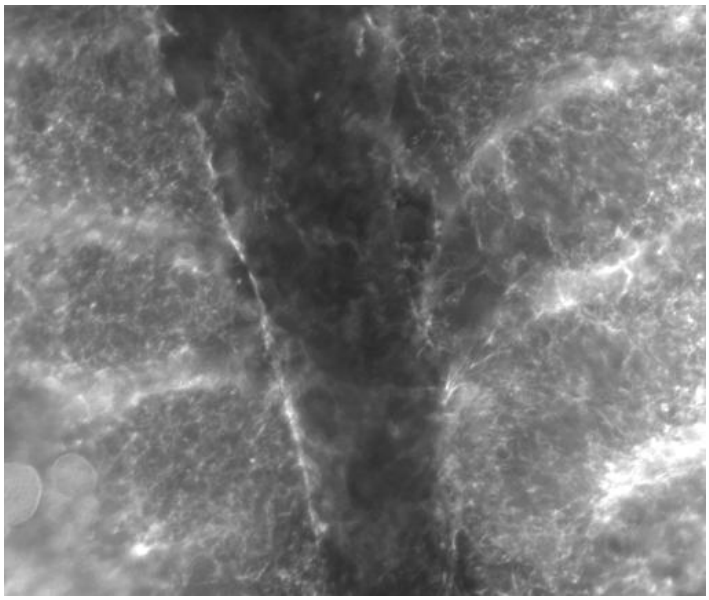

Figure 13: The lateral distribution of fibronectin network in a stage 8 embryo

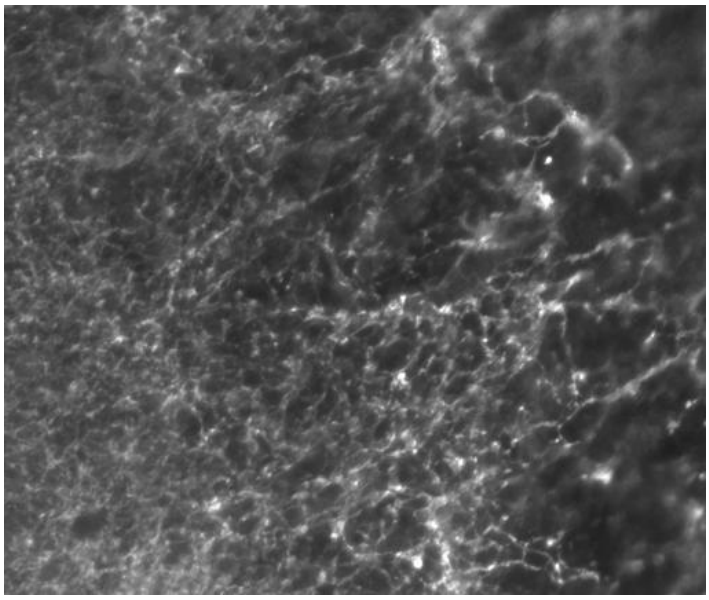

During stage 9, the medial fibronectin network is primarily composed of the somitic

fibers thickened at the edges demarcating individual somites (figure 14). However, the lateral fibronectin at stage 9 closely follows the primary vascular patterns that form in the following few hours of embryonic development (figure 15).

Figure 14: The medial distribution of fibronectin network in a stage 9 embryo

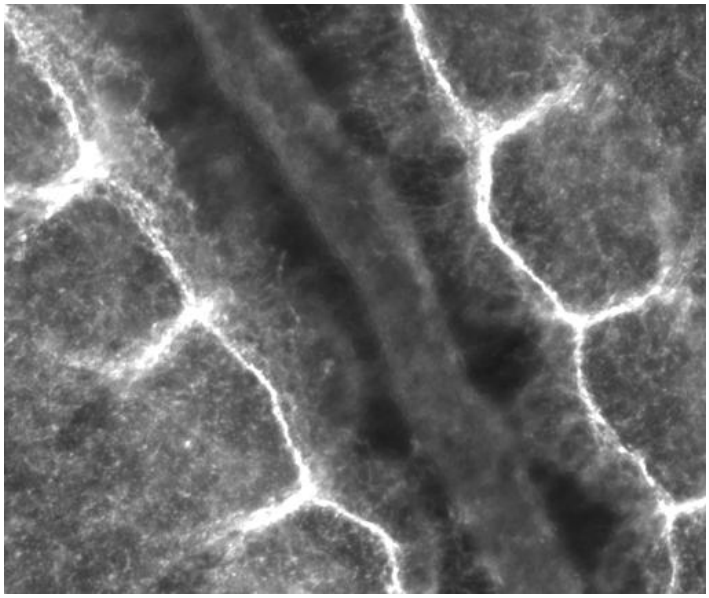

Figure 15: The lateral distribution of fibronectin network in a stage 9 embryo

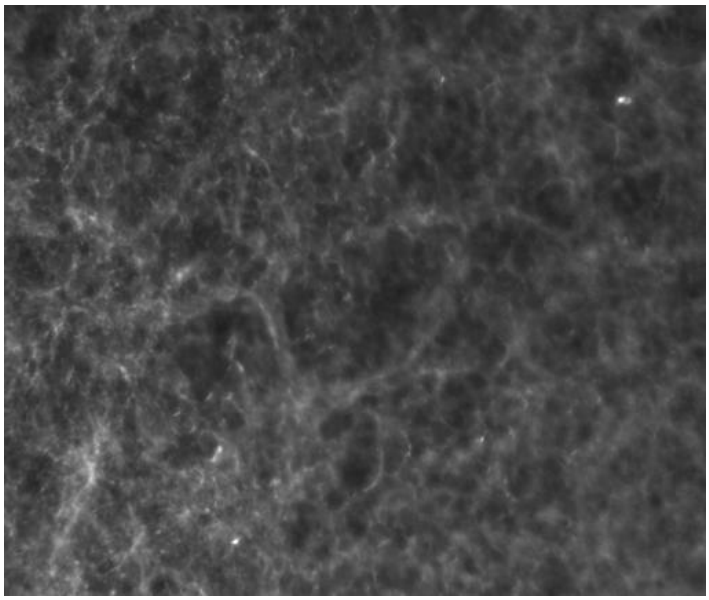

From the GLCM, the textural features were obtained and plotted as shown in the following pages of this section. The figures on contrast, correlation, energy and homogeneity were obtained by plotting the textural features as a function of the multidirectional directional offsets from two samples. The figures for the local entropic maps are shown for a representative sample only although the plots on textural entropy shown in the analysis section was obtained from the results of two embryos for medial and lateral fibronectin distributions.

Contrast or Inertia or Variance

Figure 16: Texture contrast of fibronectin as a function of offset in a stage 5 embryo

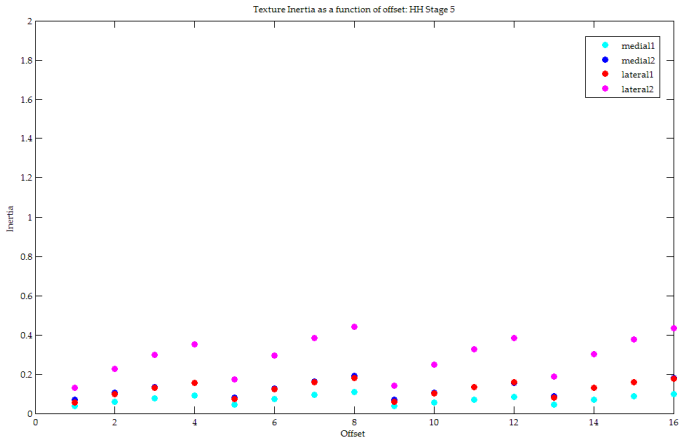

Figure 17: Texture contrast of fibronectin as a function of offset in a stage 6 embryo

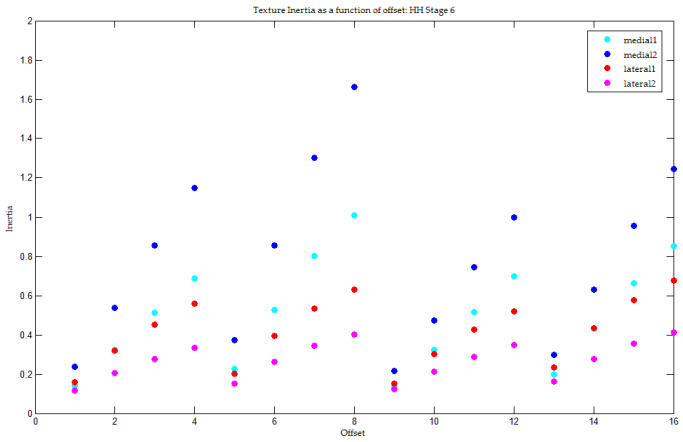

Figure 18: Texture contrast of fibronectin as a function of offset in a stage 7 embryo

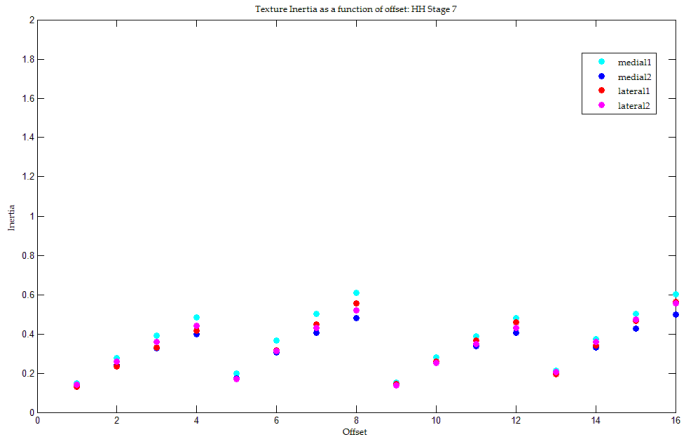

Figure 19: Texture contrast of fibronectin as a function of offset in a stage 8 embryo

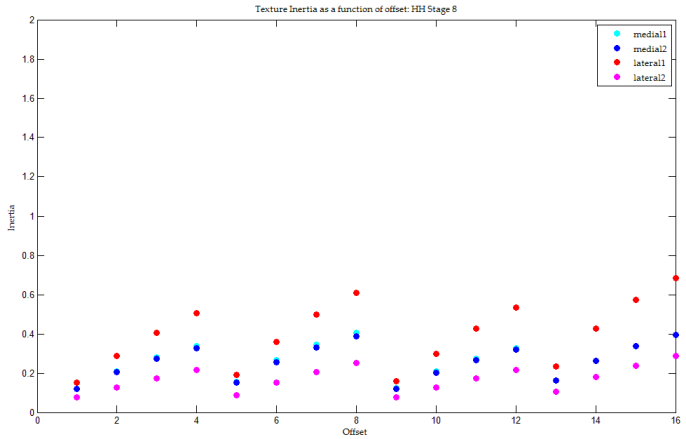

Figure 20: Texture contrast of fibronectin as a function of offset in a stage 9 embryo

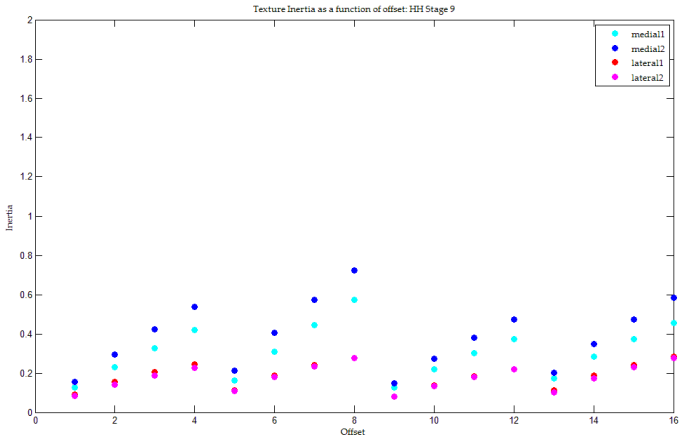

Correlation

Figure 21: Texture correlation of fibronectin as a function of offset in a stage 5 embryo

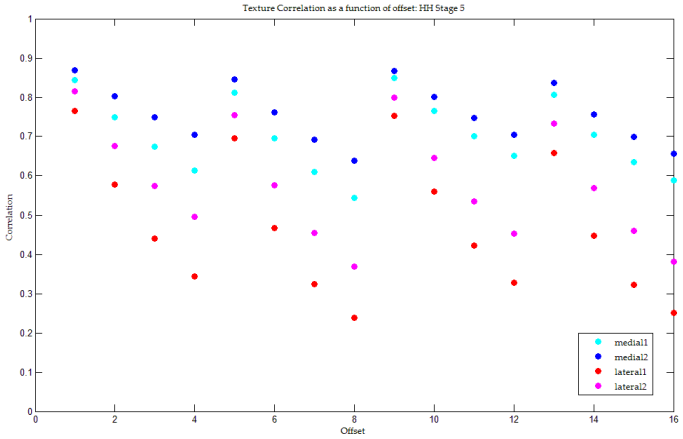

Figure 22: Texture correlation of fibronectin as a function of offset in a stage 6 embryo

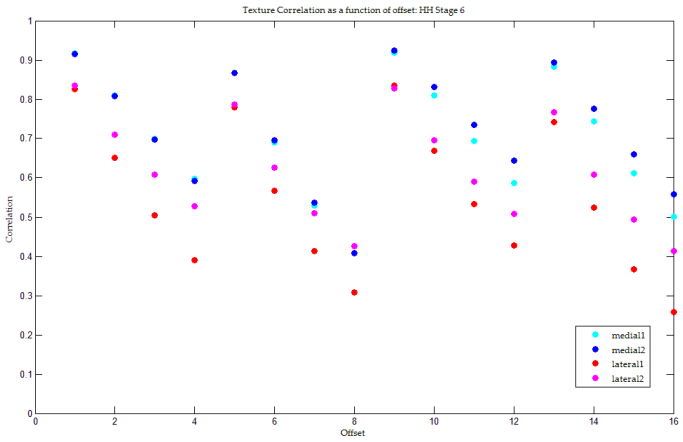

Figure 23: Texture correlation of fibronectin as a function of offset in a stage 7 embryo

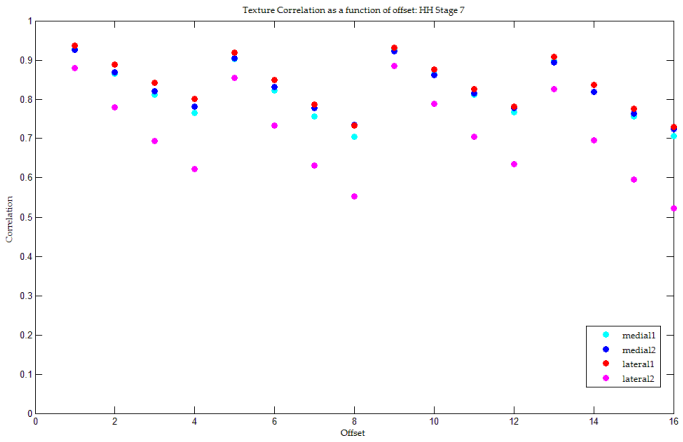

Figure 24: Texture correlation of fibronectin as a function of offset in a stage 8 embryo

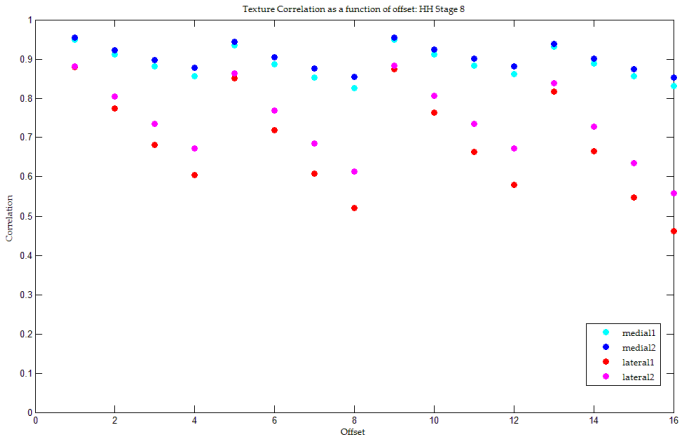

Figure 25: Texture correlation of fibronectin as a function of offset in a stage 9 embryo

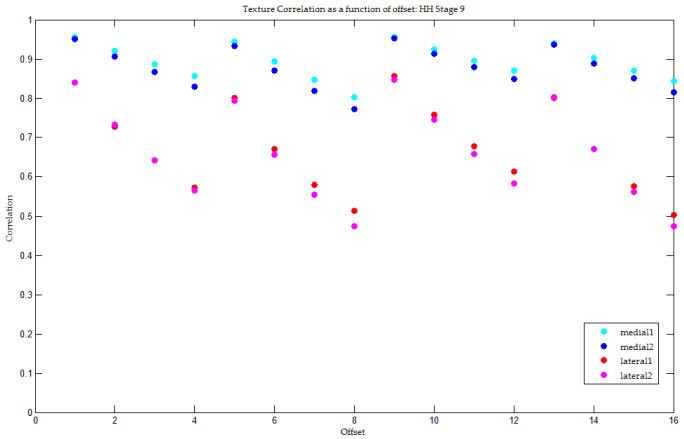

Energy or Uniformity

Figure 26: Texture uniformity of fibronectin as a function of offset in a stage 5 embryo

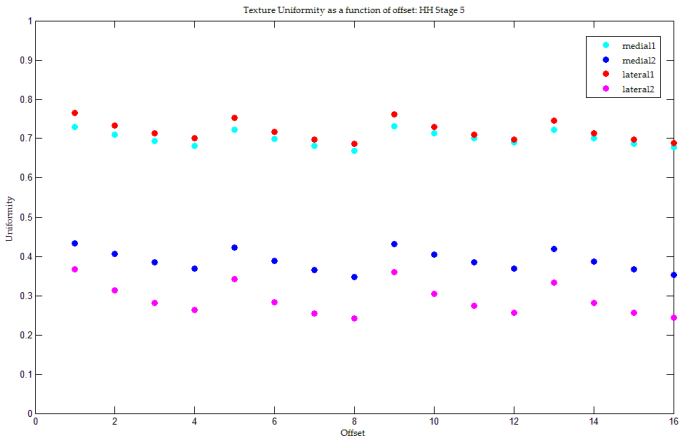

Figure 27: Texture uniformity of fibronectin as a function of offset in a stage 6 embryo

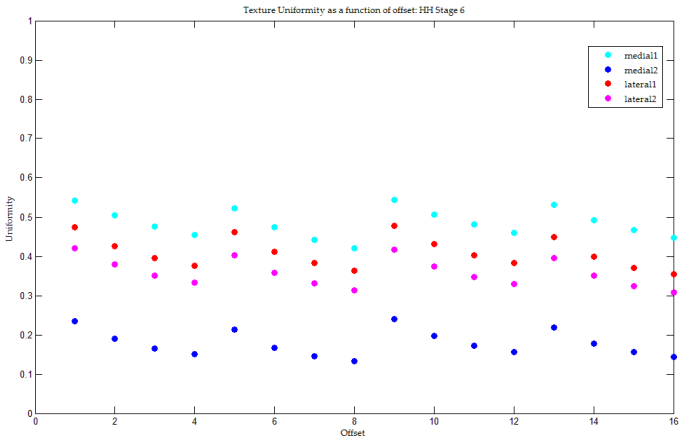

Figure 28: Texture uniformity of fibronectin as a function of offset in a stage 7 embryo

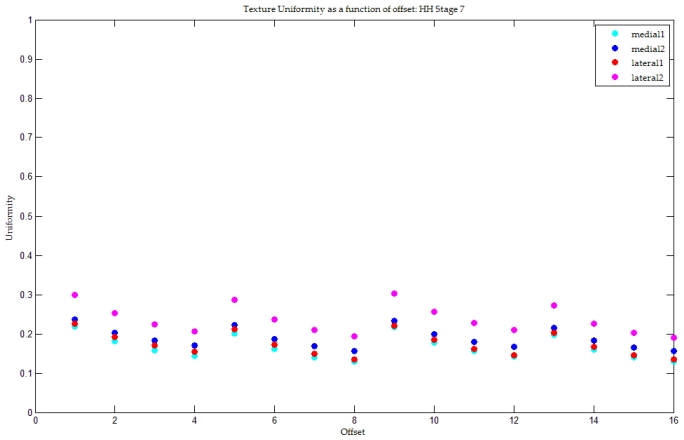

Figure 29: Texture uniformity of fibronectin as a function of offset in a stage 8 embryo

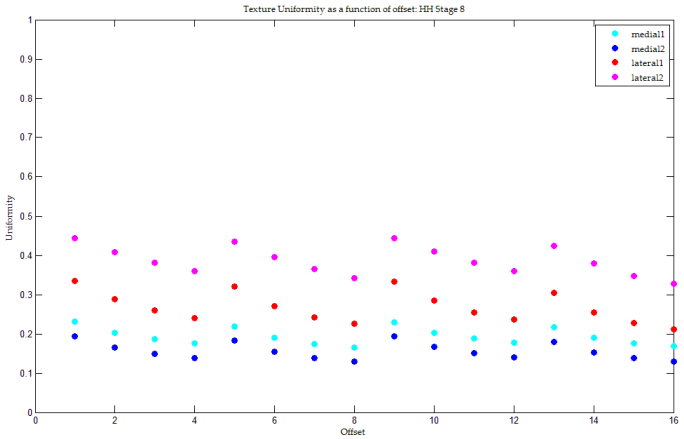

Figure 30: Texture uniformity of fibronectin as a function of offset in a stage 9 embryo

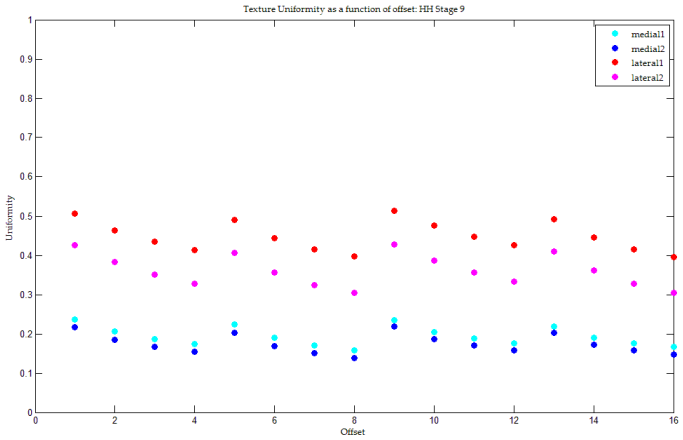

Entropy

Figure 31: Local texture entropy map of the medial fibronectin network in a stage 5 embryo

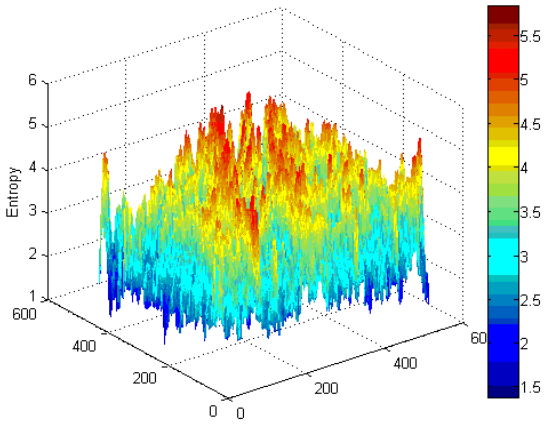

Figure 32: Local texture entropy map of the lateral fibronectin network in a stage 5 embryo

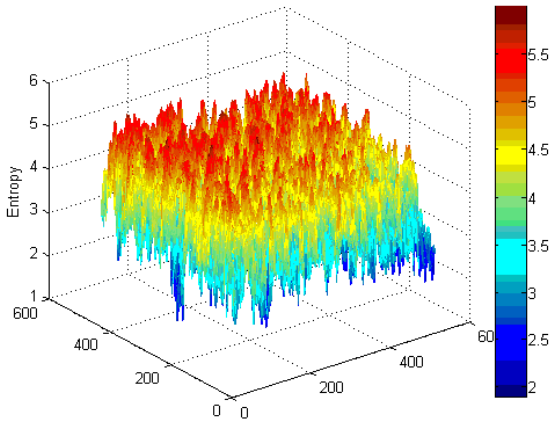

Figure 33: Local texture entropy map of the medial fibronectin network in a stage 6 embryo

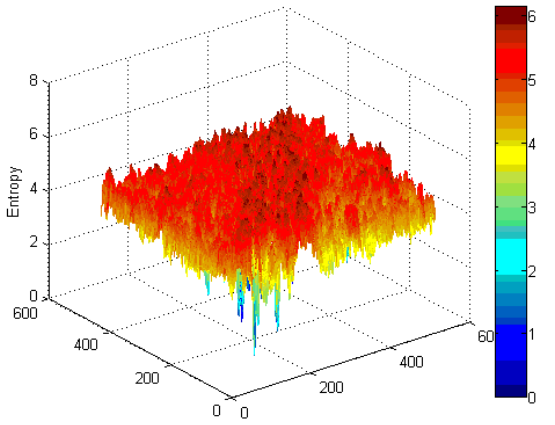

Figure 34: Local texture entropy map of the lateral fibronectin network in a stage 6 embryo

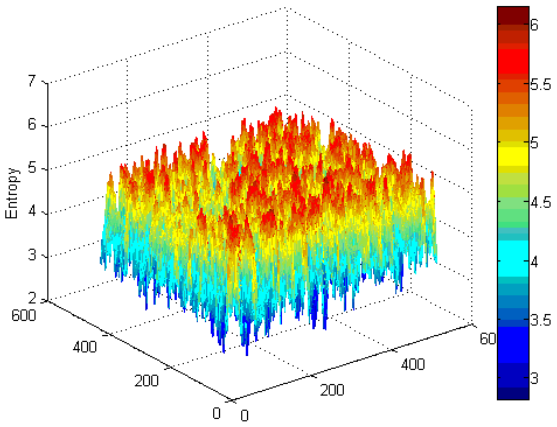

Figure 35: Local texture entropy map of the medial fibronectin network in a stage 7 embryo

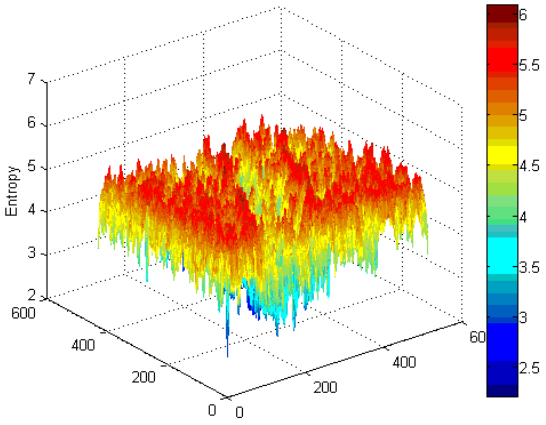

Figure 36: Local texture entropy map of the lateral fibronectin network in a stage 7 embryo

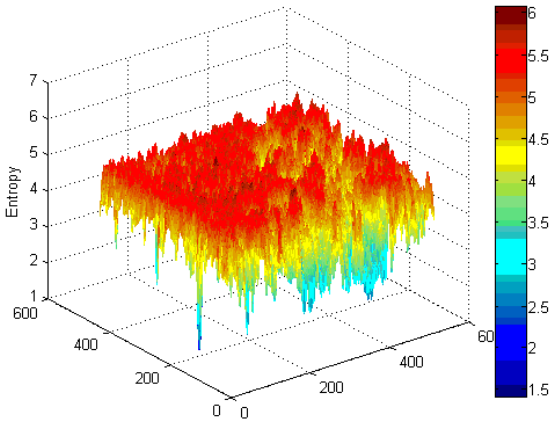

Figure 37: Local texture entropy map of the medial fibronectin network in a stage 8 embryo

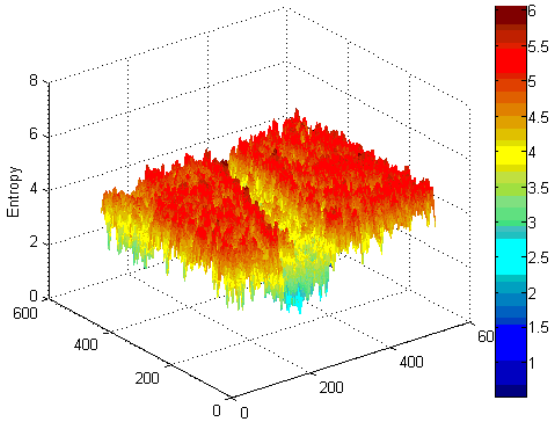

Figure 38: Local texture entropy map of the lateral fibronectin network in a stage 8 embryo

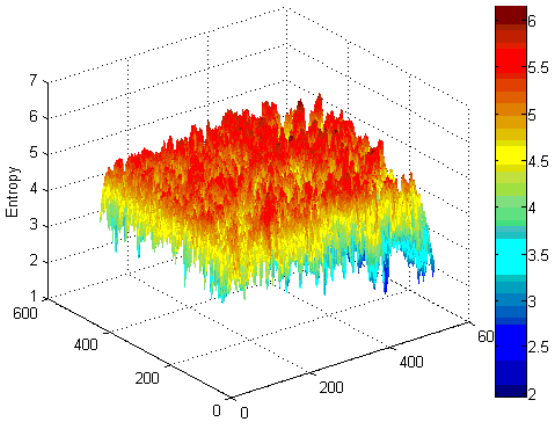

Figure 39: Local texture entropy map of the medial fibronectin network in a stage 9 embryo

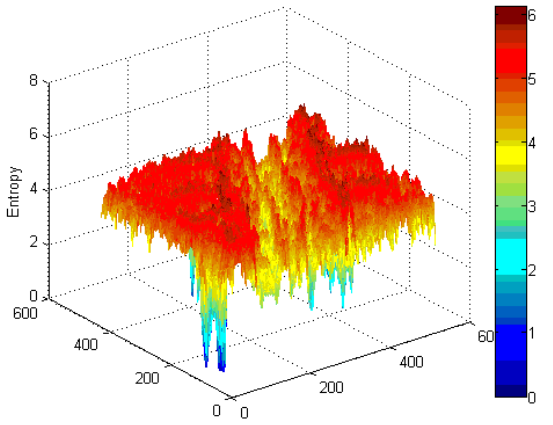

Figure 40: Local texture entropy map of the lateral fibronectin network in a stage 9 embryo

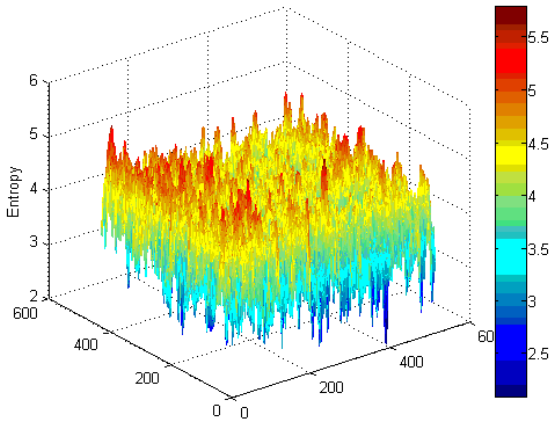

Homogeneity

Figure 41: Texture homogeneity of fibronectin as a function of offset in a stage 5 embryo

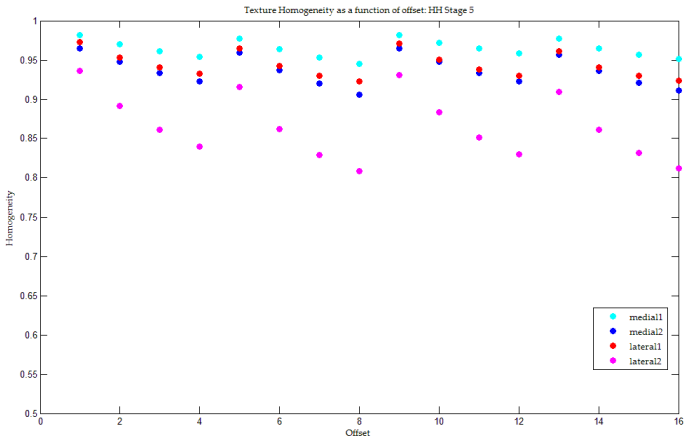

Figure 42: Texture homogeneity of fibronectin as a function of offset in a stage 6 embryo

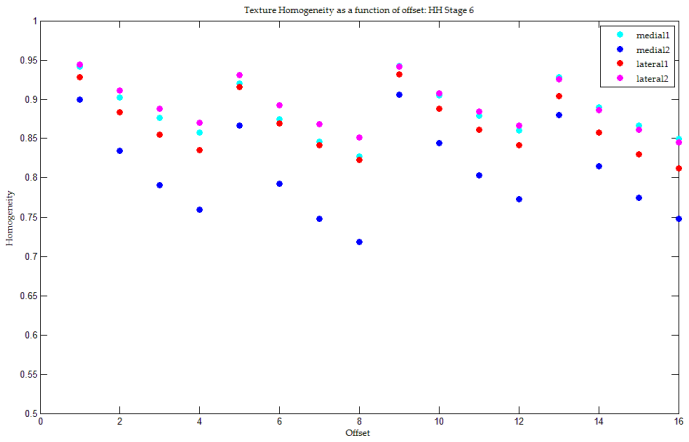

Figure 43: Texture homogeneity of fibronectin as a function of offset in a stage 7 embryo

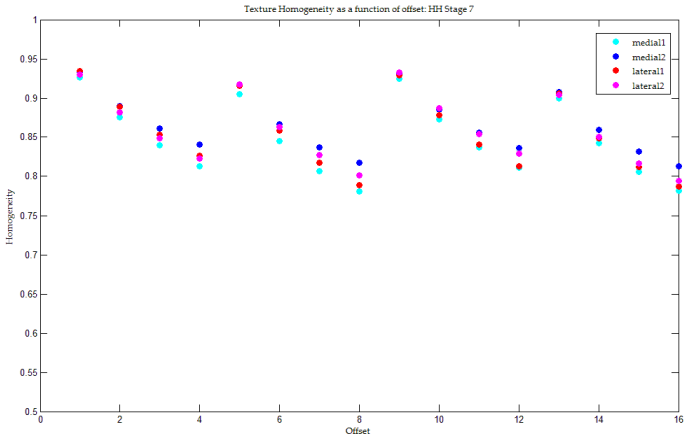

Figure 44: Texture homogeneity of fibronectin as a function of offset in a stage 8 embryo

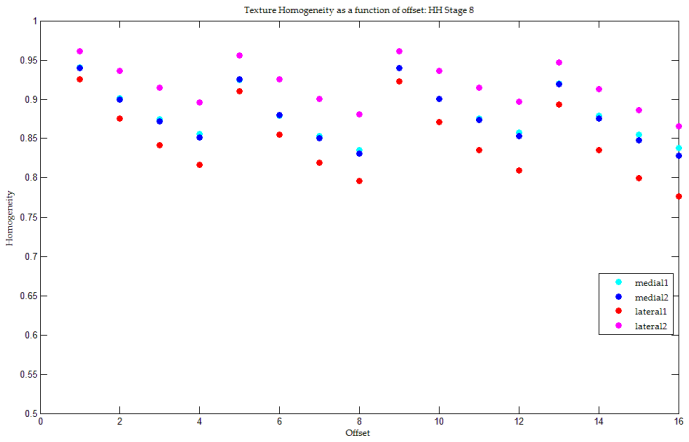

Figure 45: Texture homogeneity of fibronectin as a function of offset in a stage 9 embryo

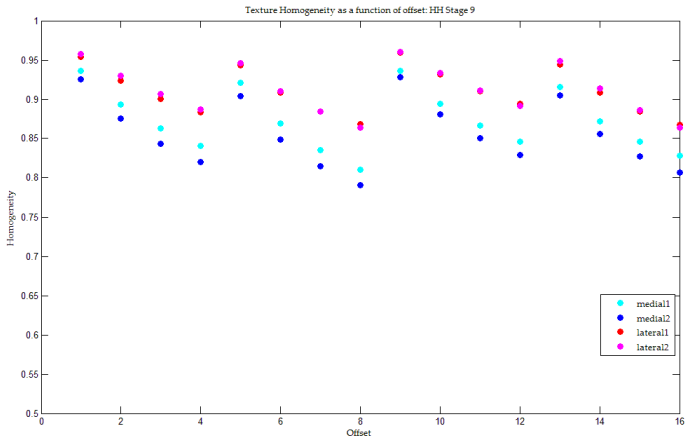

Analysis

Based on the four directional offset set up for the GLCM following the example of Haralick et. al [Haralick, 1972], the above textural parameters were obtained. In particular, contrast, correlation, energy and homogeneity were obtained for 16 offsets. Based on these values, a relative qualitative expression for the texture of fibronectin distribution was obtained as summarized in figure 46. The textural parameters were also verified for similar trends with a fully horizontal offset up to 500 values with which the above mentioned trend for the 16 offsets were compared. The plots of textural properties clearly demonstrate a measurable anisotropy in textural features of the medial and lateral fibronectin distributions. Interestingly, for the stages studied, the regional textural differences were not remarkably different in stage 7 embryos suggesting that not all the stages of development undergo textural heterogeneity in matrix distribution. Perhaps, the developmental events occurring during stage 7 require a homogenous matrix texture along the entire medial-lateral embryonic plane for normal development, an example of a local region captured during this analysis. Shown below is a plot (figure 46) of the entropic features of medial versus lateral fibronectin distributions as they evolve over time during the embryonic development.

Figure 46: Temporal evolution of textural entropy (mean value from two samples) as the embryo develops from stage 5 through stage 9

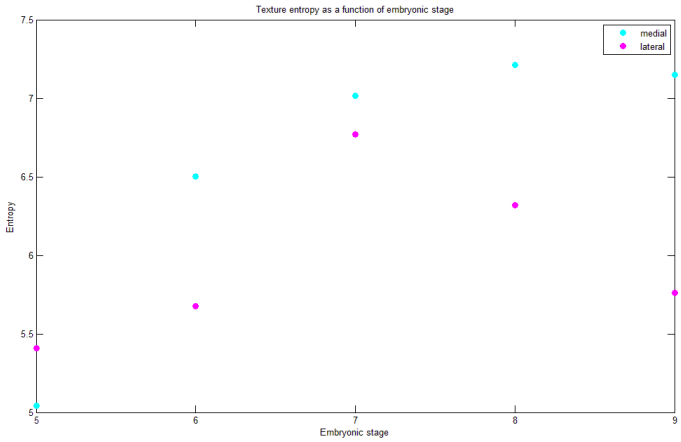

The use of two samples and the resulting lack of adequate statistical power (0.80) did not enable a traditional t-test for difference between means with a probability level of significance held at 0.05. Meanwhile, the trend was clear with the current results and presumably could be expected to hold upon addition of more samples during future investigations. With a non-conservative P value of 0.3, thus allowing a 30% probability for the detection of textural entropic differences between the medial and lateral fibronectin distribution by chance alone, a textural timing diagram (figure 47 in the summary section) was obtained to represent the qualitative texture of fibronectin based on entropy and energy (inversely related textural parameters).

The following table provides the 95% confidence interval values for the the entropy values plotted in figure 46, along with the level of significance obtained by student's t-test for difference between means $\pm$ standard error for n =2.

Stage	Confidence Interval for mean entropy difference between the medial and lateral fibronectin distributions	P value
5	-1.388 to 0.651	0.26
6	-0.989 to 2.639	0.189
7	-0.985 to 1.473	0.484
8	-0.371 to 2.156	0.093
9	0.253 to 2.527	0.034

In terms of the functional relevance of the textural analysis results in the context of embryology, few conjectures could be made. It is evident from the analysis that there exists a relative difference in the values of textural parameters of fibronectin depending on the embryonic regions under consideration. Whether these variations in matrix texture translate to differences in the mechanical properties of the matrix is yet to be explored. The regional variations in mechanical properties (textural properties) of matrix molecules have profound ramifications for cellular behavior both during normal

physiology (e.g., embryonic development) and pathology (e.g., cancer metastasis). A previous study has shown that the physical properties of fibronectin matrix determined by the dynamics of fiber assembly are highly important for normal embryonic development [Rozario,2009,386]. Moreover, cells have been shown to prefer a smooth to rough (or stiff) matrix for migrational trends observe *in vitro* [Lo, 2000, 144], a phenomenon described as durotaxis. In the context of embryonic development, it was also shown that cells might utilize information from a similar phenomenon called haptotaxis [Poole, 1982, 144]. While there have been multiple reports on the existence of multiple sources of information in the form of gradients across the embryonic volumes that provide signals to the cells (chemotaxis, galvanotaxis, haptotaxis, and perhaps durotaxis), whether texture gradients are also part of this array of information is yet to be seen. Based on the results of this study, the concept of "texturotaxis" appears worthy of further exploration.

Chapter 6: Summary

In summary, this thesis was the first attempt to explore the possible application of texture analysis to characterize an extracellular matrix network in the context of developmental biology. The results of this work has provided the necessary evidence, by serving as an example, to pursue future explorations in applying the texture analysis tools for characterization of matrix molecular networks both in health and disease. In the context of embryology, this study has demonstrated the possibility of existence of textural anisotropy with regard to fibronectin during early development. Since normal fibronectin structure and function are essential to the normal development of vascular and neural systems in the embryo, the results showing textural spatial (within the embryo for a given stage of development) and temporal (within a given region across the stages of development) anisotropy in fibronectin distribution perhaps have ramifications for developmental biology.

As shown in figure 47, a textural timing diagram can be used to summarize the qualitative descriptions that capture the textural properties of the matrix molecule.

Figure 47: Texture timing diagram of a fibronectin network from embryonic stages 5 through 9

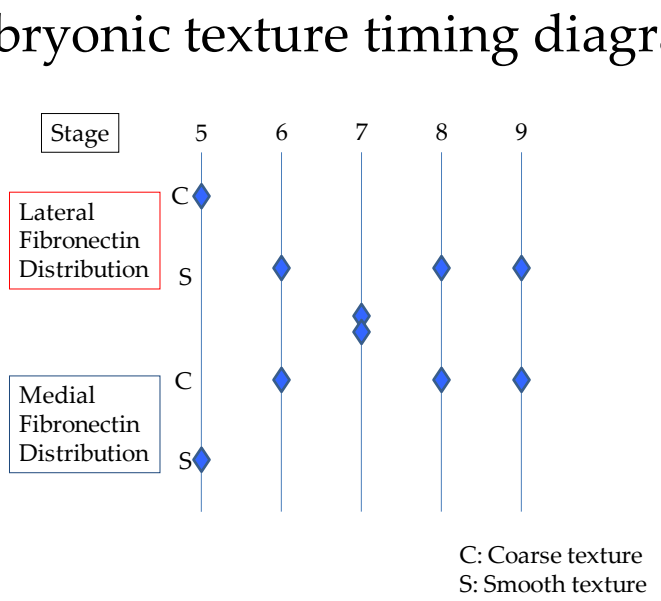

These results demonstrated that the gray scale co-occurrence matrix method of determining textural properties was sensitive enough to recognize textural anisotropies within an embryo. The study also showed that the relative fibronectin textural differences fluctuate between the medial and lateral regions over the time. Within a given stage of development, there are regional variations (textural anisotropies). An example of a local mediolateral textural homogeneity was first identified at stage 7.

Limitations and future work

This thesis has number of limitations, mostly due to the lack of previous work related to this area of application to texture analysis. As a result, the analysis was restricted to a "representational" set of input images. A future study may utilize a rigorous statistical approach for the characertization of matrix texture not only at the medial and lateral regions of the embryo, but also the entire embryonic distribution of fibronectin. Meanwhile, to capture the *in vivo* scenario completely the analysis might be extended to other matrix molecules such as fibrillin, collagen, laminin etc. that also play a crucial role in embryonic development. In addition the analysis of matrix texture could be extended to pathological tissues as well. Texture analysis has already found applications in cancer histopathology. As mentioned in the summary, investigation of evidence towards the possibility of textural gradients in the extracellular matrix and their importance in cell biology could lead to important biological insights and will provide us tools to control cell behavior in tissue engineering applications. Finally, a major limitation of this study was that it captured a "snap shot" analysis of fibronectin distribution during development of an embryo (a highly dynamic biological process). In order to truly capture the in vivo scenario, tools need to be developed (future work) to allow an analysis of dynamic textural changes of extracellular matrix during embryonic development.

References

1. [George, 1993, 1079] George EL et al. Defects in mesoderm, neural tube and vascular development in mouse embryos lacking fibronectin. Development. 1993 Dec; 119(4):1079-91.

2. [Zamir,2006,19806] Zamir EA et al. Mesodermal cell displacements during avian gastrulation are due to both individual cell-autonomous and convective tissue movements. Proc Natl Acad Sci USA. 2006, Dec 26; 103(52): 19806-11.

3. [Zamir, 2008, e247] Zamir EA et al. The ECM moves during primitive streak formation – computation of ECM versus cellular motion. PLoS Biol. 2008 Oct 14: 6(10):e247

4. [Czirok, 2008, 269] Czirok A et al. Multicellular sprouting during vasculogenesis. Curr Top Dev Biol. 2008; 81: 269 – 89.

5. [Rozario,2009,386] Rozario T et al. The physical state of fibronectin matrix differentially regulates morphogentic movements in vivo. Dev Biol. 2009 Mar 15; 327(2): 386-98.

6. [Lo, 2000, 144] Lo CM et al. Cell movement is guided by the rigidity of the substrate. Biophys J. 2000 Jul; 79(1): 144-52.

7. [Vakonakis, 2007, 578] Vakonakis I and Campbell ID. Extracellular matrix: from atomic resolution to ultrastructure. Curr Opin Cell Biol. 2007 Oct; 19 (5): 578-83.

8. [Rovasio, 1983, 462] Rovasio et al. Neural crest cell migration: requirements for exogenous fibronectin and high cell density. J Cell Biol. 1983 Feb; 96(2): 462-73.

9. [Duband, 1986, 160] Duband et al. Cell adhesion and migration in the early vertebrate embryo: location and possible role of the putative fibronectin complex. J Cell Biol. 1986 Jan; 102(1): 160-78.

10. [Vakaet, 1962, 38] Vakaet L. Some new data concerning the formation of the definitive endoblast in the chick embryo. J Embryol Exp Morphol. 1962 Mar; 10: 38-57.

11. [Duband, 1982,337] Duband JL and Thiery JP. Appearance and distribution of fibronectin during chick embryo gastrulation and neurulation. Dev Biol. 1982 Dec; 94(2):337-50.

12. [Sanders, 1982, 155] Sanders EJ. Ultrastructural immunocytochemical localization of fibronectin in the early chick embryo. J Embryol Exp Morphol. 1982 Oct; 71: 155-70.

13. [Mitrani, 1982, 197] Mitrani E and Farberov AU. Fibronectin expression during the process leading to axis formation in the chick embryo. Dev Biol. 1982 May; 91(1): 197 – 201.

14. [Newgreen, 1980, 269] Newgreen D and Thiery JP. Fibronectin in early avian embryos: synthesis and distribution along the migration pathways of neural crest cells. Cell Tissue Res. 1980; 211(2): 269-91.

15. [Duband, 1982, 308] Duband JL and Thiery JP. Distribution of fibronectin in the early phase of avian cephalic neural crest migration. Dev Biol. 1982 Oct; 93(2):308-23.

16. [Thiery, 1982, 324] Thiery JP et al. Pathways and mechanisms of avian trunk neural crest cell migration and localization. Dev Biol. 1982 Oct; 93(2):324-43.

17. [Vincent, 1984, 468] Vincent M and Thiery JP. A cell surface marker for neural crest and placodal cells: further evolution in peripheral and central nervous system. Dev Biol. 1984 Jun; 103(2):468-81.

18. [Bronner-Fraser, 1985, 610] Bronner-Fraser M. Alterations in neural crest migration by a monoclonal antibody that affects cell adhesion. J Cell Biol. 1985 Aug; 101(2): 610-7.

19. [Critchley,1979, 498] Critchley DR et al. Distribution of fibronectin in the ectoderm of gastrulating chick embryos. Nature. 1979 Aug 9; 280(5722):498-500.

20. [Chiquet, 1981, 220] Chiquet M et al. Muscle Morphogenesis: Evidence for an organizing function of exogenous fibronectin. Dev Biol. 1981 Dec; 88(2):220-35.

21. [Risau, 1988, 441] Risau W and Lemmon V. Changes in vascular extracellular matrix during embryonic vasculogenesis and angiogenesis. Dev. Biol. 1988 Feb;125(2):441-50.

22. [Drake,1990, 309] Drake CJ et al. Avian vasculogenesis and the distribution of collagens I, IV, laminin, and fibronectin in the heart primordial. J Exp Zool. 1990 Sep; 255(3): 309-22.

23. [Rupp,2001,566] Rupp PA and Little CD. Integrins in vascular development. Circ Res. 2001 Sep 28; 89(7):566-72.

24. [Thiery, 1984, 1] Thiery JP. Mechanisms of cell migration in the vertebrate embryo. Cell Differ. 1984 Nov; 15(1): 1-15.

25. [Böttcher RT, 2005, 63] Böttcher RT and Niehrs C. Fibroblast growth factor signaling during early vertebrate development. Endocr Rev. 2005 Feb; 26(1):63-77.

26. [Affolter M,2005, 19] Affolter M and Weijer CJ. Signaling to cytoskeletal dynamics during chemotaxis. Dev Cell. 2005 Jul; 9(1):19-34.

27. [Vasiev, 2010,e10571] Vasiev B et al. Modeling gastrulation in the chick embryo: formation of the primitive streak. PLoS One. 2010 May 11; 5(5):e10571.

28. [Poole, 1982, 144] Poole TJ and Steinberg MS. Evidence for the guidance of pronephric duct migration by a craniocaudally travelling adhesion gradient. Dev Biol. 1982 Jul; 92(1): 144-58.

29. [Tuceryan, 1998, 207] Tuceryan M and Jain AK. Texture analysis. In the handbook of pattern recognition and computer vision (2nd edition), by C.H. Chen, L. F. Pau, P.S.P.Wang (eds.), pp.207-248, World Scientific Publishing Co., 1998.

30. [Julesz, 1962, 84] Julesz B. Visual pattern discrimination, IRE Trans on Information Theory, IT-8, 1962, pp. 84-92.

31. [Julesz, 1981, 91] Julesz B. Textons, the elements of texture perception, and their interactions. Nature. 1981 Mar 12; 290(5802):91-7.

32. [Haralick, 1979, 786] Haralick RM. Statistical and structural approaches to texture. Proceedings of the IEEE, Vol. 67, No. 5, May 1979, 786 – 804.

33. [Carlucci, 1972, 53] Carlucci L. A formal system for texture languages. Pattern Recognition, vol. 4, 1972, pp. 53-72.

34. [Haralick, 1972, 12-2-1] Haralick RM et al. On some quickly computable features for texture. Proc. 1972 symp. On comput. Image Processing and Recognition (Univ. of Missouri, Columbia, MO), vol. 2, Aug 1972, pp 12-2-1 to 12- 2- 10.

35. [Dewaele, 1988, 56] Dewaele P et al. Texture inspection with self-adaptive convolution filters. Proc. of the 9th international conference on pattern recognition, 1988, pp. 56 – 60.

36. [Conners,1983, 573] Conners RW et al. Identifying and locating surface defects in wood: Part of an automated lumber processing system. IEEE trans. on pattern analysis and machine intelligence, PAMI-5, 1983, pp.573-583.

37. [Siew, 1988, 105] Siew LH et al. Texture measures for carpet wear assessment. IEEE trans. on pattern analysis and machine intelligence, PAMI-10, 1988, pp.92-105.

38. [Jain, 1990, 1] Jain AK et al. Texture analysis of automotive finishes. Proc. of SME Machine Vision Applications Conference, Nov. 1990, pp. 1-16

39. [Sutton, 1972, 667] Sutton R and Hall EL. Texture measurements for automatic classification of pulmonary disease. IEEE Trans on Computers, C-21, 1972, pp. 667-676.

40. [Doyle, 2008, 496] Doyle S et al. Automated grading of breast cancer histopathology using spectral clustering with textural and architectural image features. 5th IEEE International Symposium on Biomedical Imaging: From Nano to Macro, 2008. ISBI 2008. pp. 496-499.

41. [Doyle, 2007, 1284] Doyle S et al. Automated grading of prostate cancer using architectural and textural image features. 4th IEEE International Symposium on Biomedical Imaging: From Nano to Macro, 2007. ISBI 2007. pp. 1284-1287.

42. [Jain, 1991, 1167] Jain AK and Farrokhnia F. Unsupervised texture segmentation using Gabor Filters. Pattern Recognition, 24, 1991, pp 1167-1186.

43. [Haralick, 1973, 610] Haralick RM et al. Textural features for image classification. IEEE transactions on systems, man and cybernetics, SMC-3, 1973, pp.610-621.

44. [Rignot, 1990, 1979] Rignot E and Kwok R. Extraction of textural features in SAR images: statistical model and sensitivity. Proc of international geoscience and remote sensing symposium, 1990, pp. 1979-1982.

45. [Du, 1990, 1983] Du LJ. Texture segmentation of SAR images using localized spatial filtering. Proc of international geoscience and remote sensing symposium, May 1992.

46. [Lee, 1990, 2005] Lee JH and Philpot WD. A spectral-texture classifier for digital imagery. Proc of international geoscience and remote sensing symposium, 1990, pp.2005-2008.

47. [Hamburger, 1992, 231] Hamburger V and Hamilton H. A series of normal stages in the development of the chick embryo. J Morphol 88: 1951, 49-92.

48. [New, 1955, 326] New D. A new technique for the cultivation of the chick embryo in vitro. J Embryol Exp Morph 3: 1955, 326-331.

49. [Little, 2000, 183] Little C and Drake C. Whole mount immunolabeling of embryos by microinjection. Meth Mol Biol 135: 2000, 183-189.

50. [Chapman,2001, 284] Chapman SC et al. Improved method for chick whole-embryo culture using a filter paper carrier. Dev Dyn 220: 2001, 284-289.

51. The early Embryology of the Chick, Patten, Third Edition, P. Blakiston's Son & Co. Inc.,1929.

52. Biology of Extracellular Matrix: A Series; Fibronectin, Edited by Deane F. Mosher, Academic Press, Inc., 1989.

53. Preferred Orientation in Deformed Metals and Rocks: An Introduction to Modern Texture Analysis, Edited by Hans-Rudolf Wenk, Academic Press, Inc., 1985.

54. Texture Analysis in Digital Images Using Image Extrema, Amrendra Singh, University of Kansas, Dissertation, 1980.

55. Molecular Biology of The Cell, Bruce Alberts et. al., Fourth Edition, Garland Science, 2002.

56. Principles of Development, Lewis Wolpert et. al., Third Edition, Oxford university Press, 2007.

57. The Mathworks Inc., "MATLAB," Available at http://www.mathworks.com/products/matlab

Supplementary Background

A Primer on Avian Gastrulation

Although gastrulation is not a topic/subtopic of discussion for the thesis, this primer on gastrulation has been provided to include some basic information on an important morphogenetic event in the early embryo that involves a fibronectin matrix network. This section may also serve as a preliminary introduction to the thesis for the non-biologist reader since it outlines the early stages of embryonic development.

After fertilization, the ovum undergoes cell divisions called cleavage before the egg is laid. At this point, the embryo is a single layer of cells arranged over the yolk (figure A). The single layer of cells is called the epiblast.

Figure 48: The bird's egg at the early stage of development consists of a single layer of cells (epiblast) over the yolk

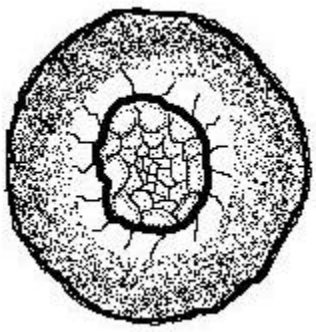

The next stage of embryonic development is marked by epiblastic cells from the future tail end of the embryo moving underneath the upper layer resulting ultimately in formation of a midline thickening of cells called the primitive streak, and also a second layer beneath the epiblast called the hypoblast. The primitive streak is the prominent midline structure visible in the embryo after approximately 16 hours of incubation of the egg (stage 4 in figure 2, and figure c). The process during which the epiblastic cells are rearranged to create a two layered embryo (epiblast & hypoblast) is called gastrulation (derived from the greek word *gaster* = stomach) referring to the fact that the cells of the hypoblast (the lower layer) give rise to the future gastric tube (stomach & intestines) of the embryo.

Figure 49: Gastrulation (side view) in a bird embryo showing the movement of epiblastic cells over the yolk (and under the epiblast) to form a second layer beneath the epiblast, called the hypoblast

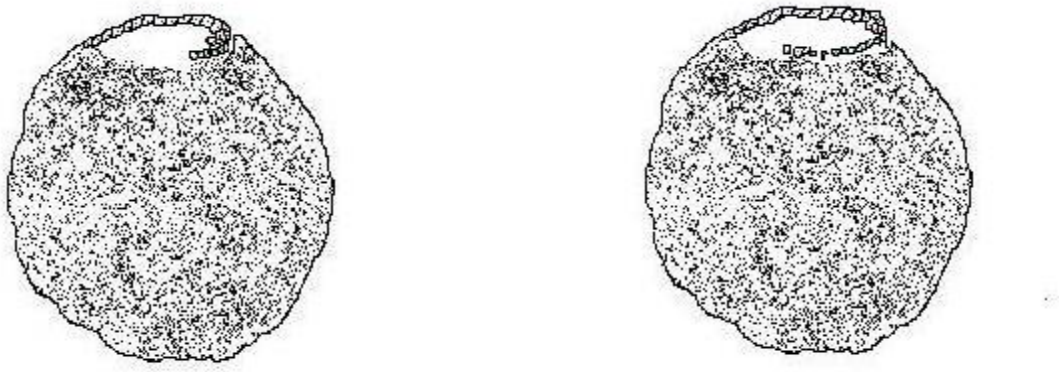

Figure 50: Appearance of the primitive streak (the midline thickening of cells from the epiblast and hypoblast) in the embryo after 16 hours of incubation of the egg (also refer to stage 4 in figure 2)

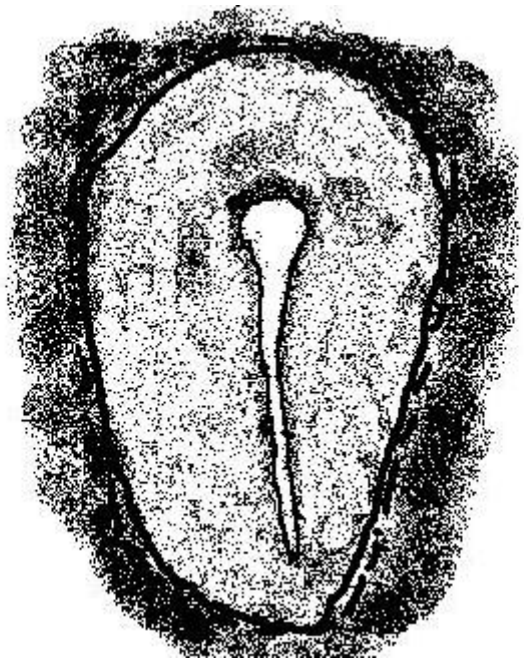

Following the development of the two layered embryo, and thickening of the cells from both the epiblastic and hypoblastic layers at the midline (primitive streak), the next stage of development involves detachment of some cells from the primitive streak and movement of these cells in between the ectoderm (upper germ layer, formerly epiblast) and endoderm (lower germ layer, formerly hypoblast) to form mesoderm, a new germ layer in the middle, made up of loosely arranged highly motile cells.

Figure 51: Median longitudinal section across the primitive streak to show the schematic of formation of the mesoderm (red). Ectoderm is in blue and Endoderm in green positioned over the yolk

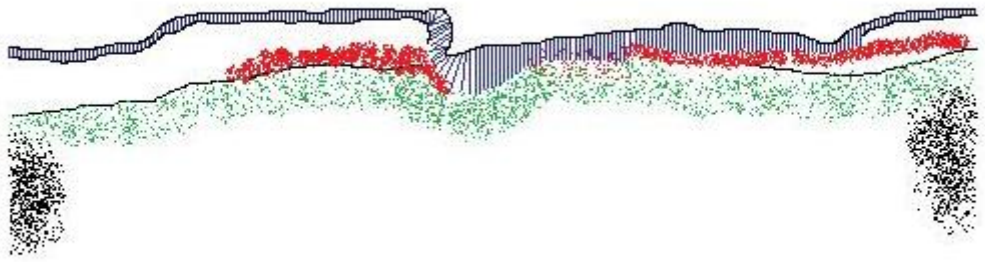

After the formation of mesoderm, the embryo has reached the point in development where it has acquired all the raw materials in the form of the three germ layers (ectoderm, mesoderm and endoderm) to provide the necessary ingredients (cell types) for the formation of organ systems. The key organs that result from ectodermal contribution are the brain, spinal cord, and skin. The Key organs/tissues that result from the mesoderm are the heart, blood vessels, blood and bones. The Key organs that result from the endoderm are, as mentioned earlier, the stomach and intestines, and also the liver, lungs and pancreas. It is precisely for this reason (future development of organ systems from the germ layers), that gastrulation as an early embryonic event holds its high significance since the formation of three germ layers is achieved via gastrulation in all animal embryos (including humans). During the movement of mesodermal cells

during gastrulation, the fibronectin matrix network (the subject of this thesis) plays a highly dynamical role in its interaction with the migratory cells.

Figure 52: A cross section of the developing embryo after gastrulation reveals the tissues developing from the three germ layers (ectoderm in blue, mesoderm in red and endoderm in green) positioned over the yolk

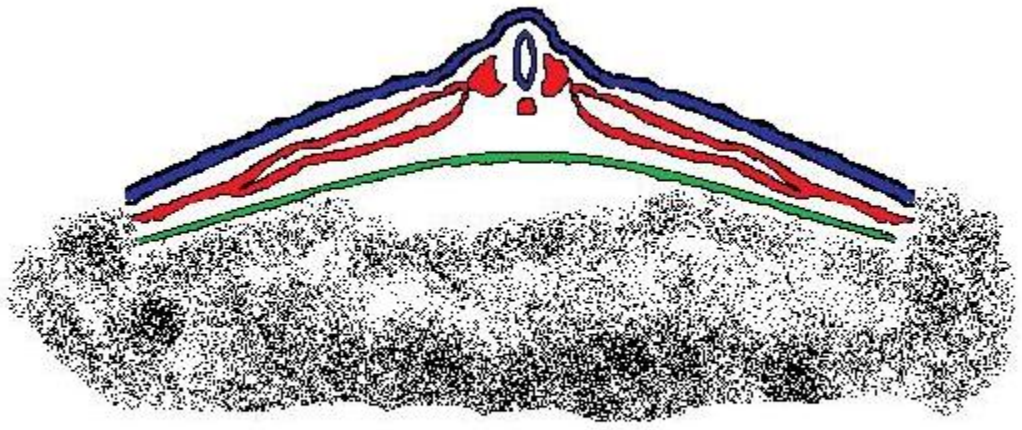

Glossary

Extracellular Matrix

Complex network of polysaccharides (sugar molecules) and proteins (such as fibronectin) secreted by cells. Serves as a structural element in tissues and influences tissue development and physiology.

First-order Statistics

FOS measure the likelihood of observing a gray value at a randomly-chosen location in the image. FOS could be computed from the histogram of pixel intensities in the image and these depend only on the individual pixel values and not on the interaction or co-occurrence of neighboring pixel values. An example of the FOS is the average intensity in the image.

Gabor Filter

A linear filter used for edge detection with frequency and orientation representations appropriate for textural analysis.

Gastrulation

The process in animal embryos in which the endoderm and mesoderm move from the outer surface of the embryo to the inside, where they give rise to internal organs. See appendix for details.

Germ layers

Refers to the regions of the early animal embryo that will give rise to distinct type of tissue. Most animals have three germ layers – ectoderm, mesoderm and endoderm. See appendix for details.

Morphogenesis

Refers to the processes (physical and chemical) involved in bringing about changes in form (embryonic anatomy) in the developing embryo.

Primitive Streak

In the bird embryo refers to the strip of cells that is the forerunner of the anterior-posterior axis. During gastrulation, the cells move through the streak into the interior of the embryo.

Quail

A small, plump, terrestrial bird in the pheasant family Phasianidae that is domesticated and farmed much like chicken.

Second-order Statistics

SOS are defined as the likelihood of observing a pair of gray values occurring at the endpoints of a dipole of random length placed in the image at a random location and orientation and are properties of pairs of pixel values.

Somites

Somites are masses of mesoderm in an early vertebrate embryo that are orderly arranged on either side of the developing neural tube and give rise to the skeletal muscle and the vertebrae.